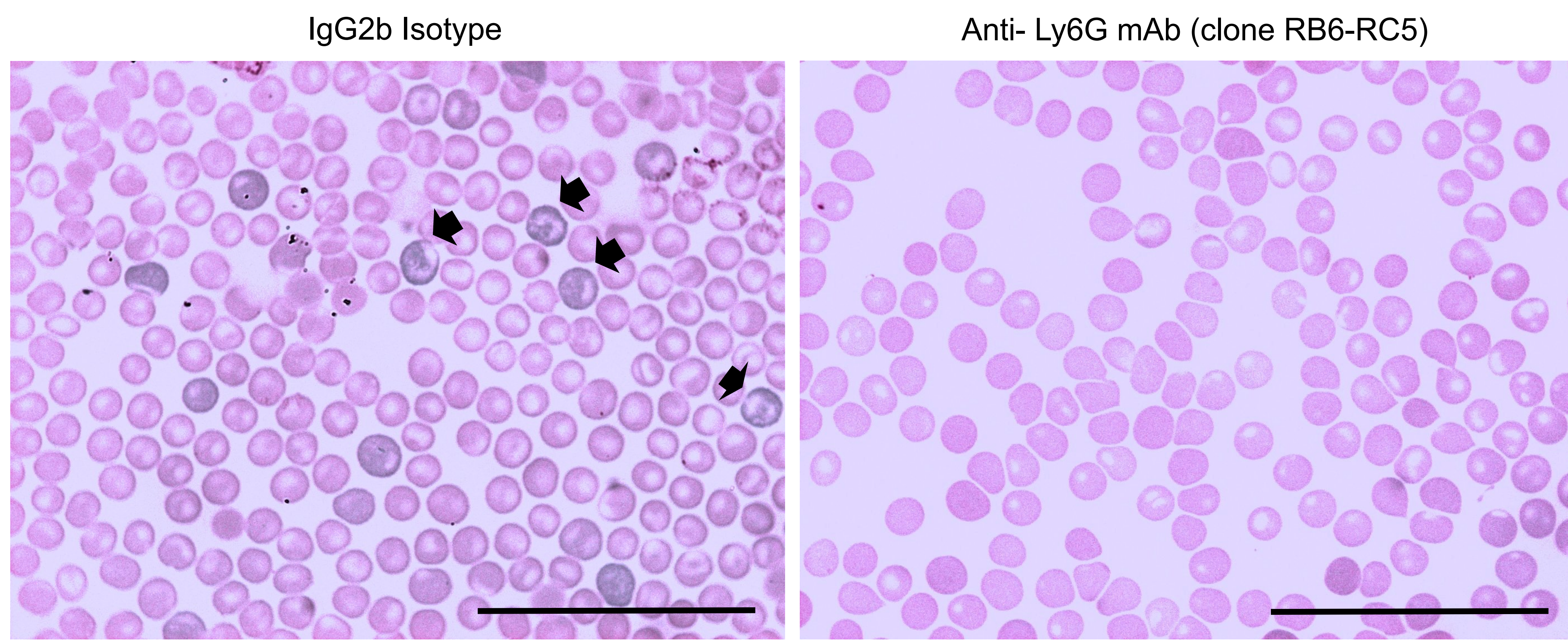
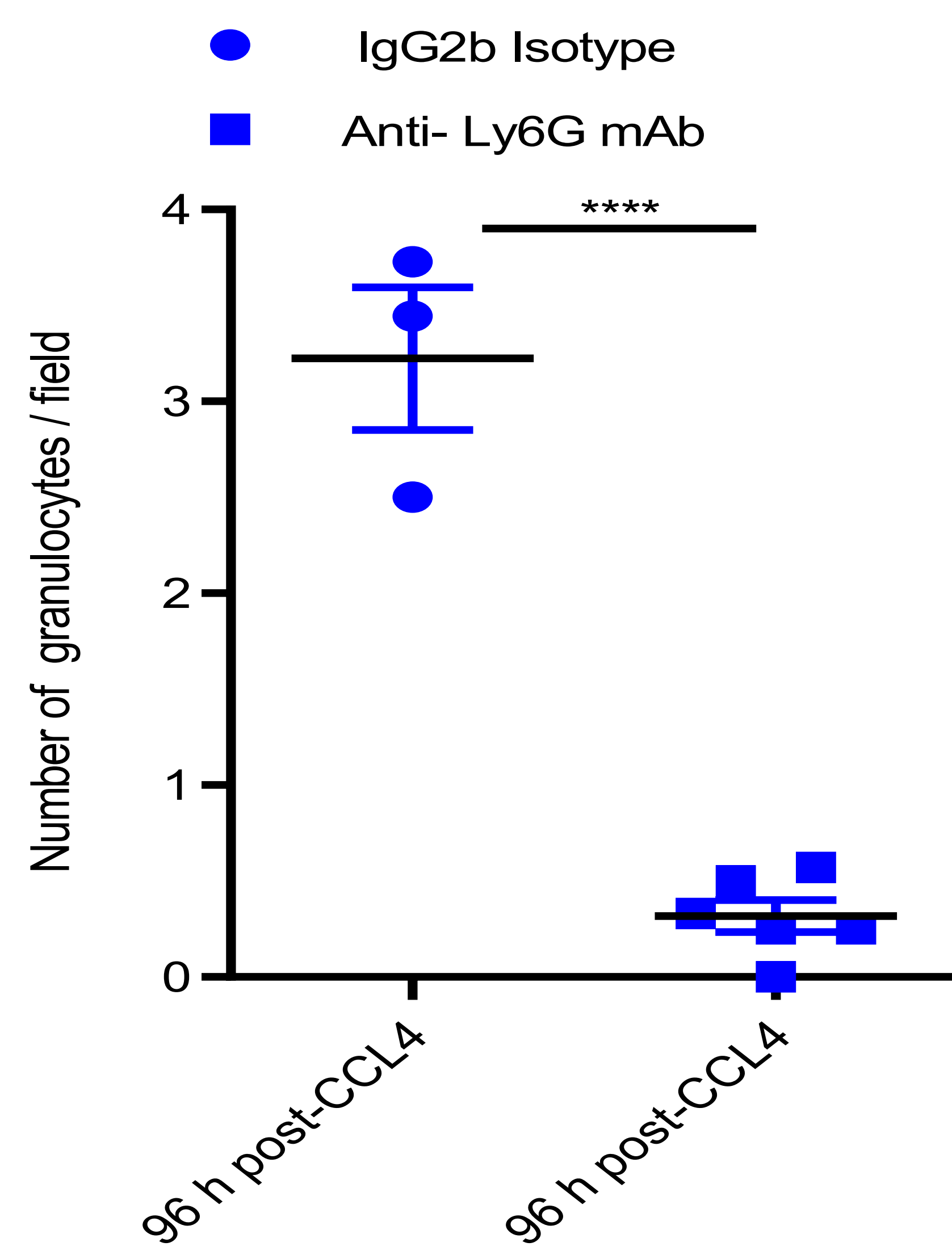


96 h post-CCL4

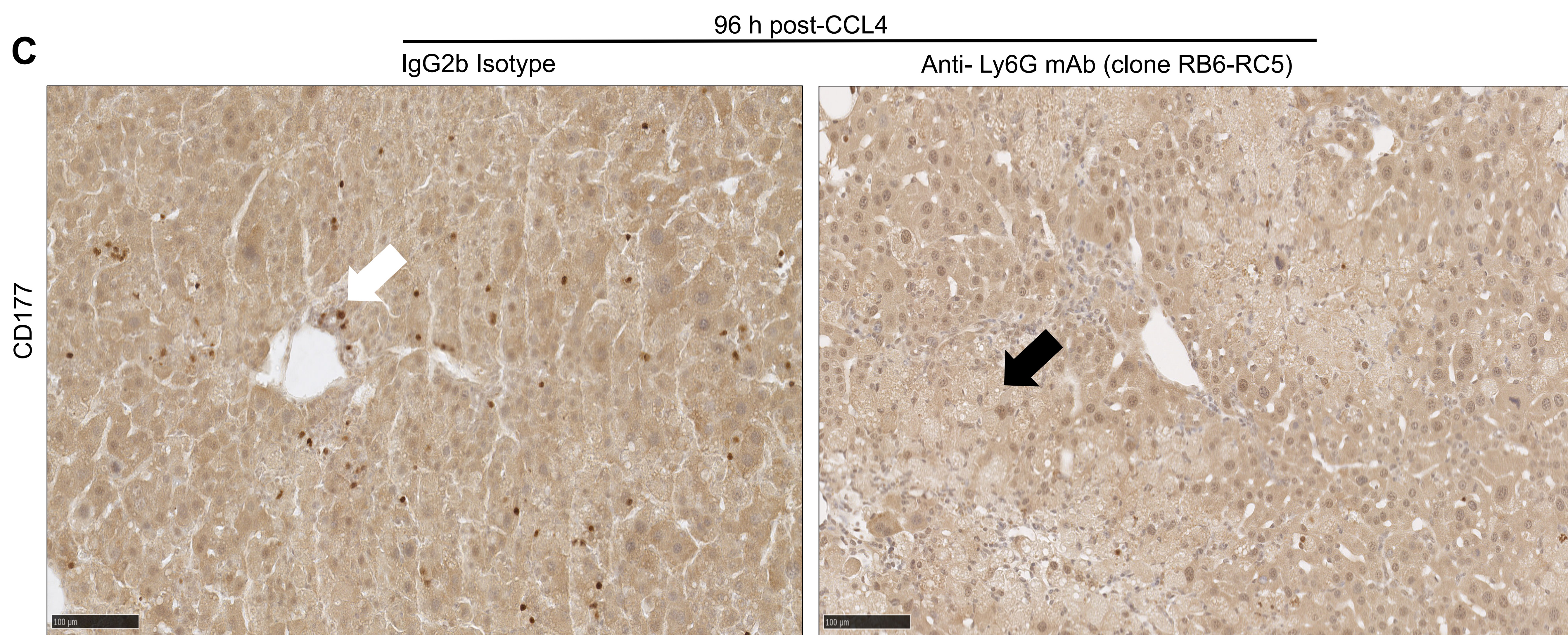
A



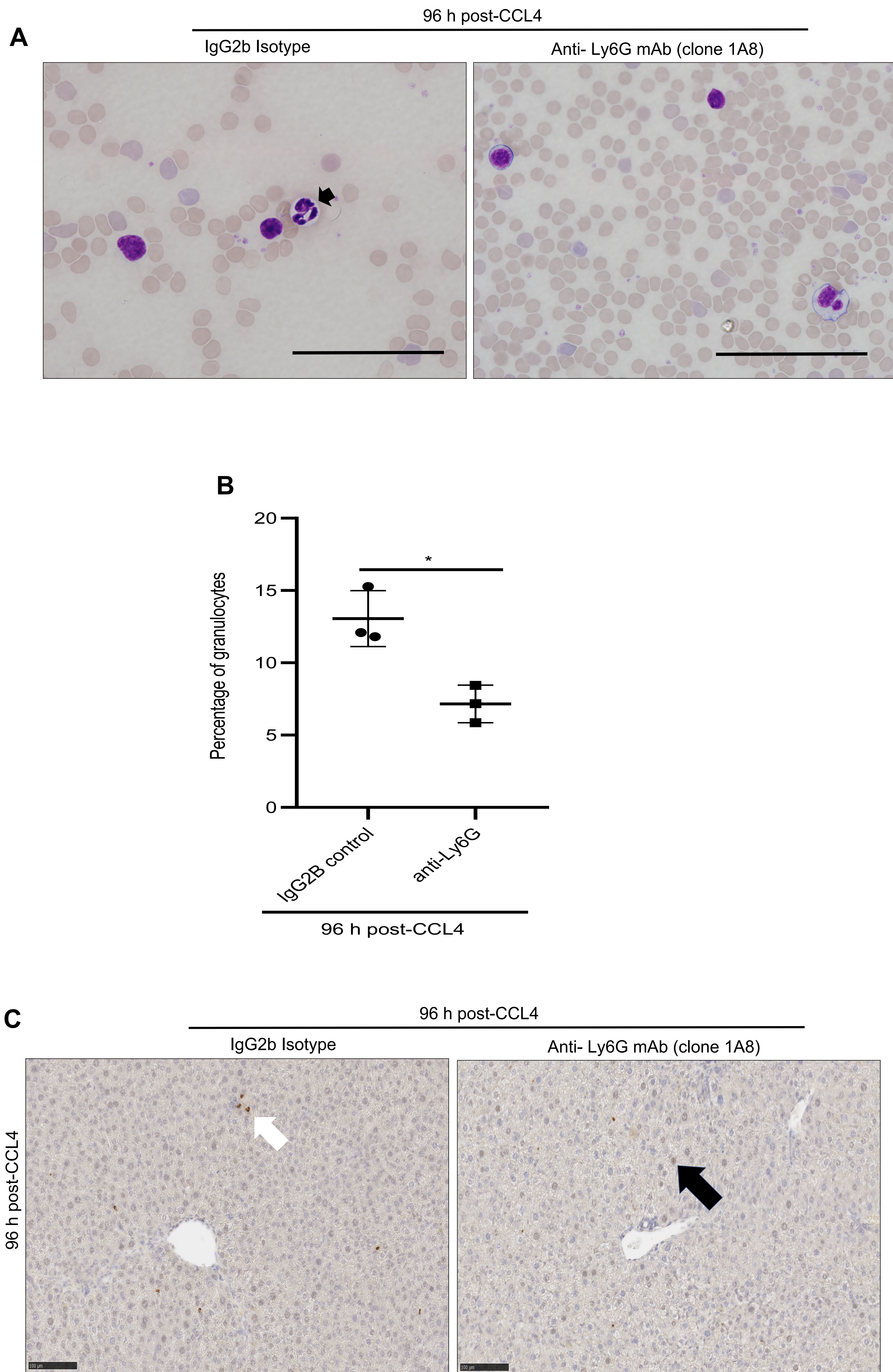
B



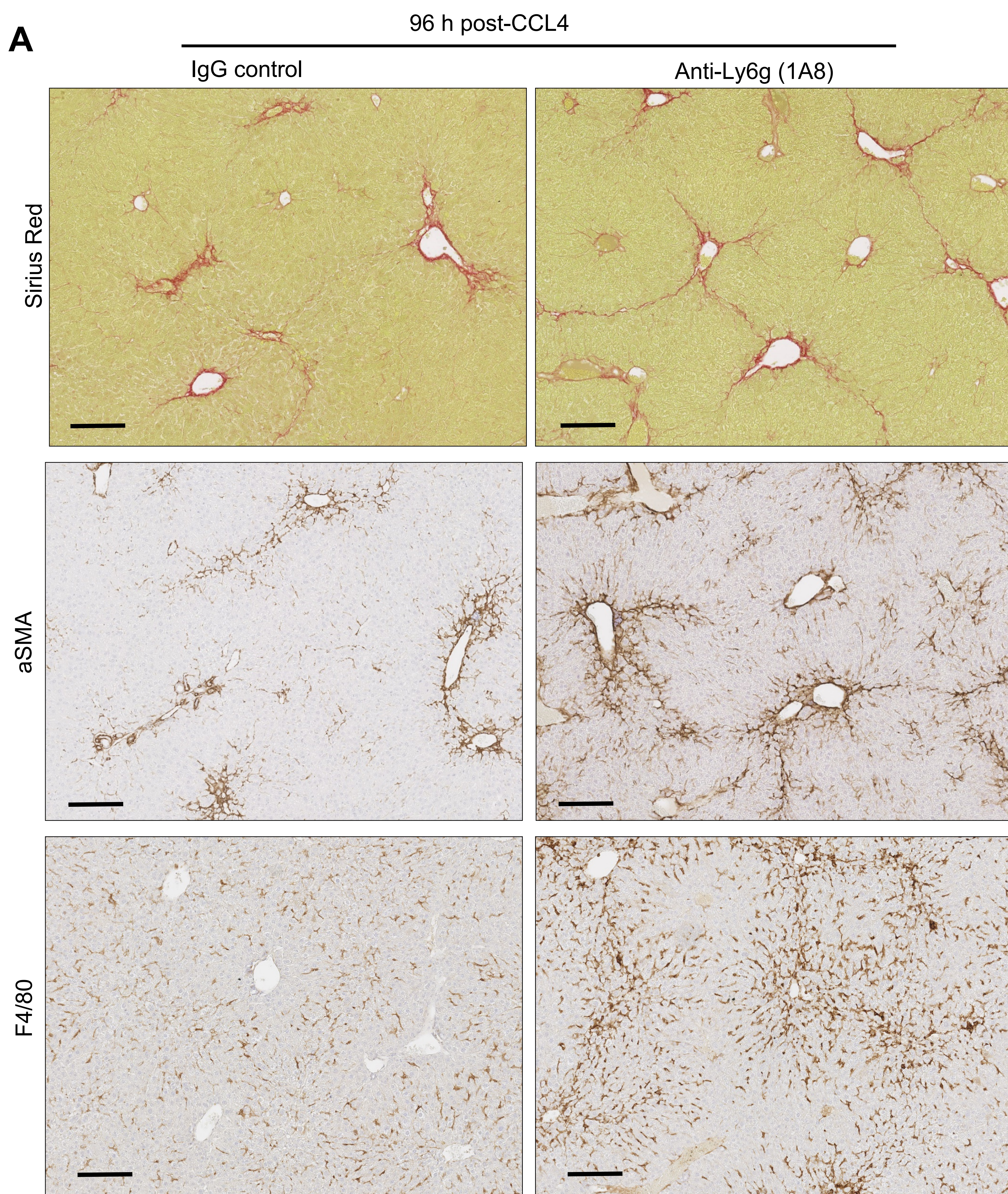
C



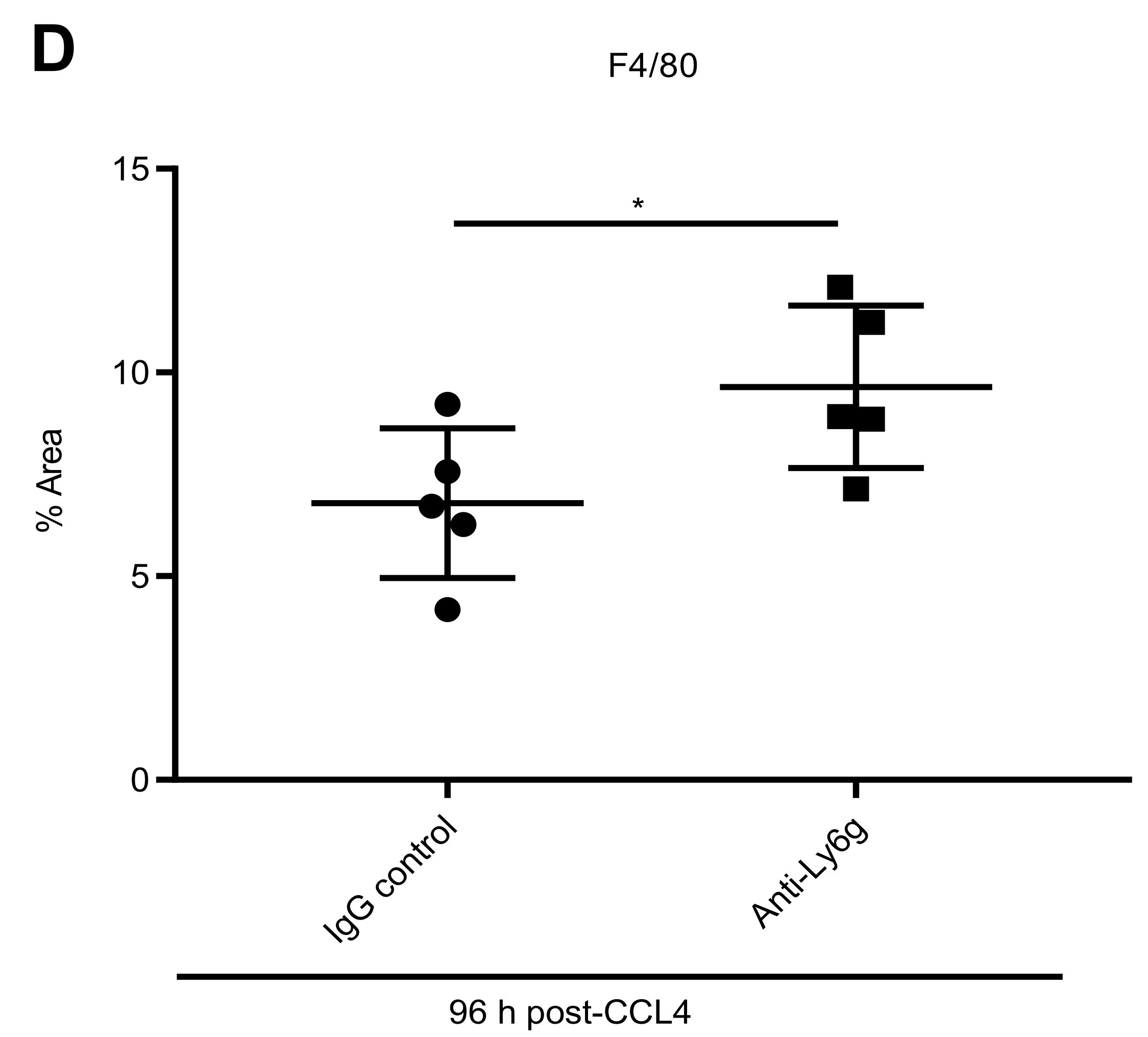
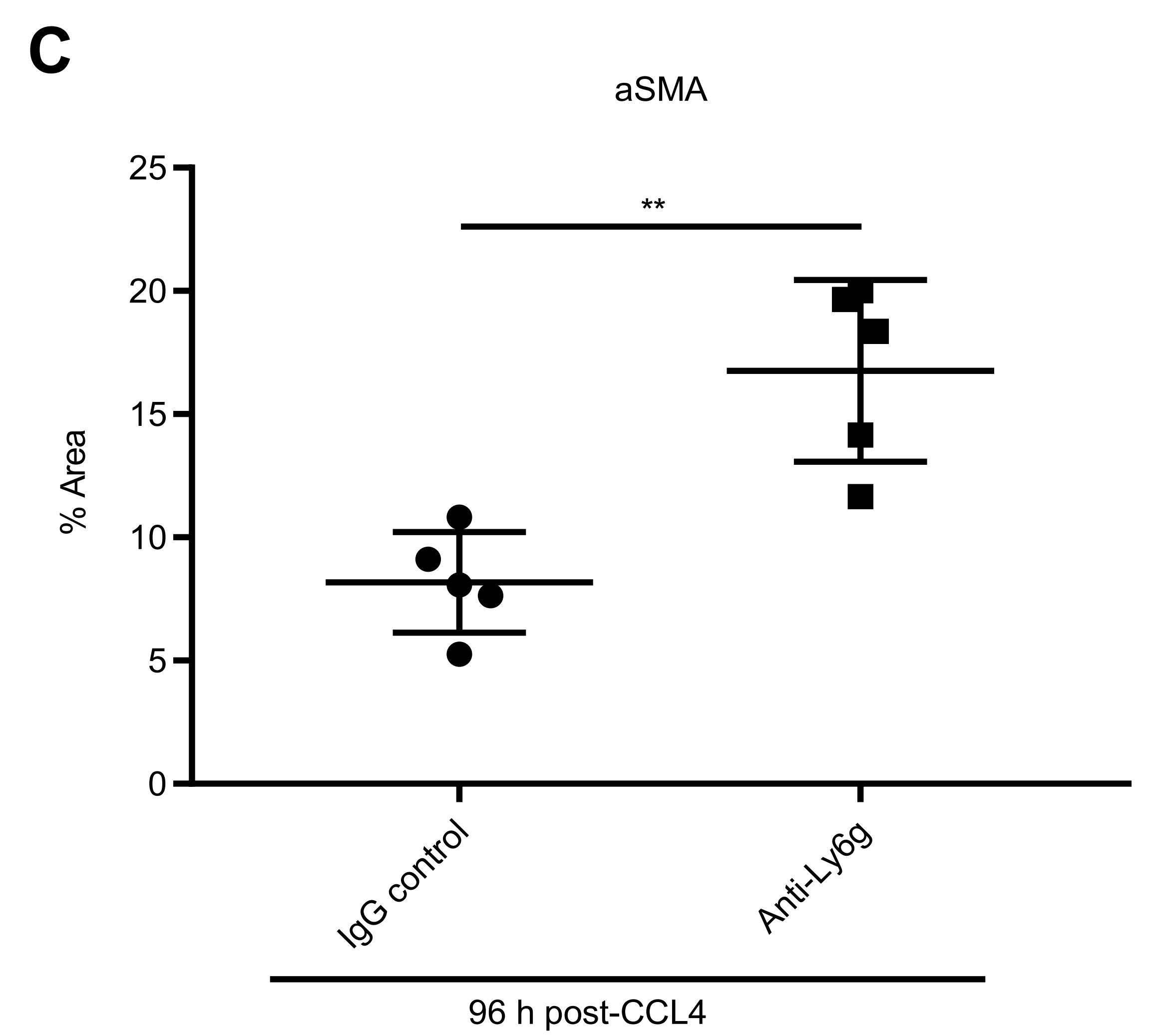
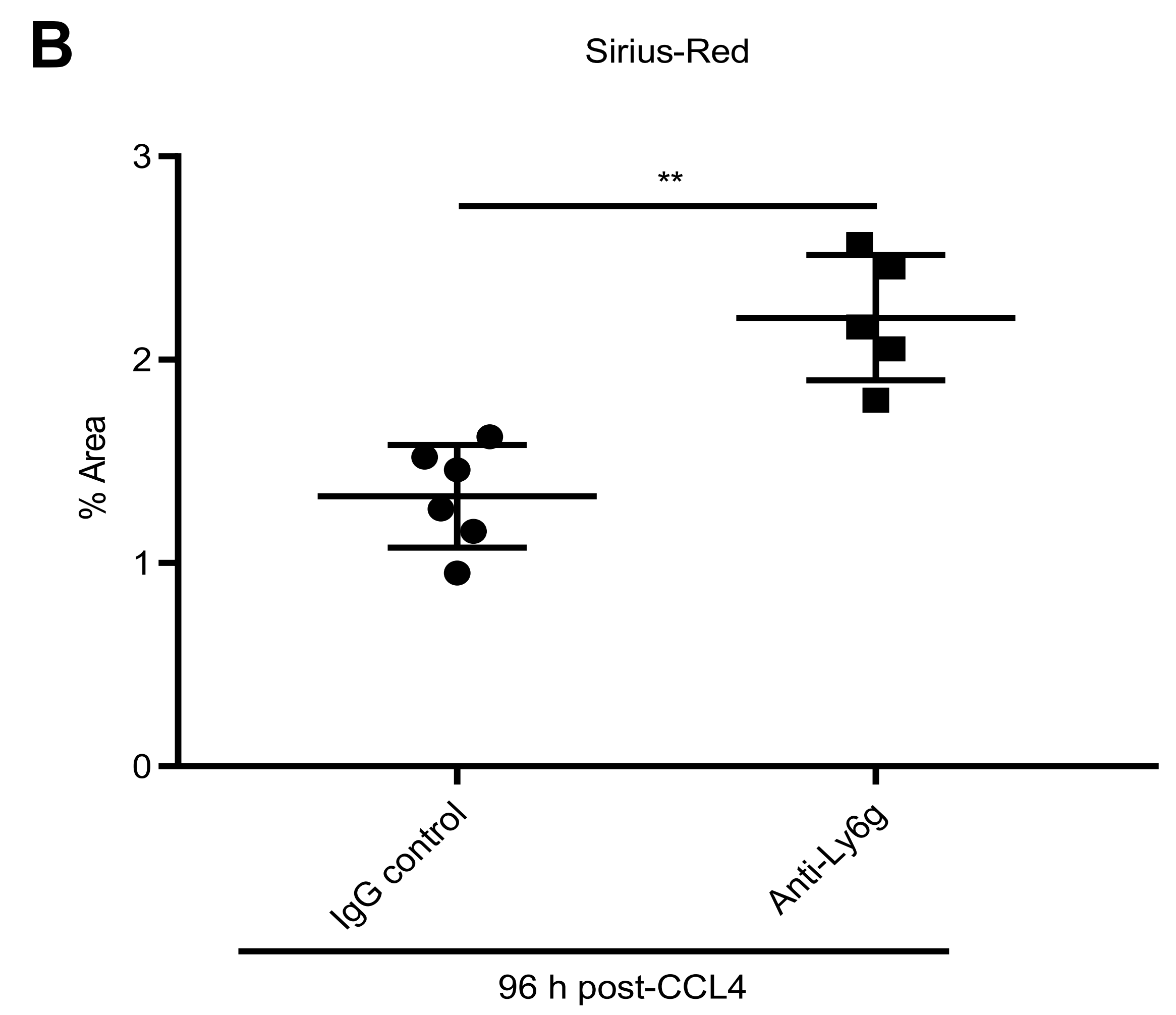
Supplementary Figure 1 (A) Representative Giemsa staining of blood smears of mice in experiment from **Figure 1 A**. Black arrows indicate stained granulocytes. Scale bars= 100 μ m. (B) Number of granulocytes per field counted manually in 10 randomly selected images; n= 3-6 . **** P <0.0001, two-tailed unpaired t-test. Data are shown as means \pm SD (C) Representative immunohistochemical images of liver neutrophils (CD177 positive). White arrows point to CD177 positive cells (neutrophils), while black arrows highlight background. Scale bars=100 μ m

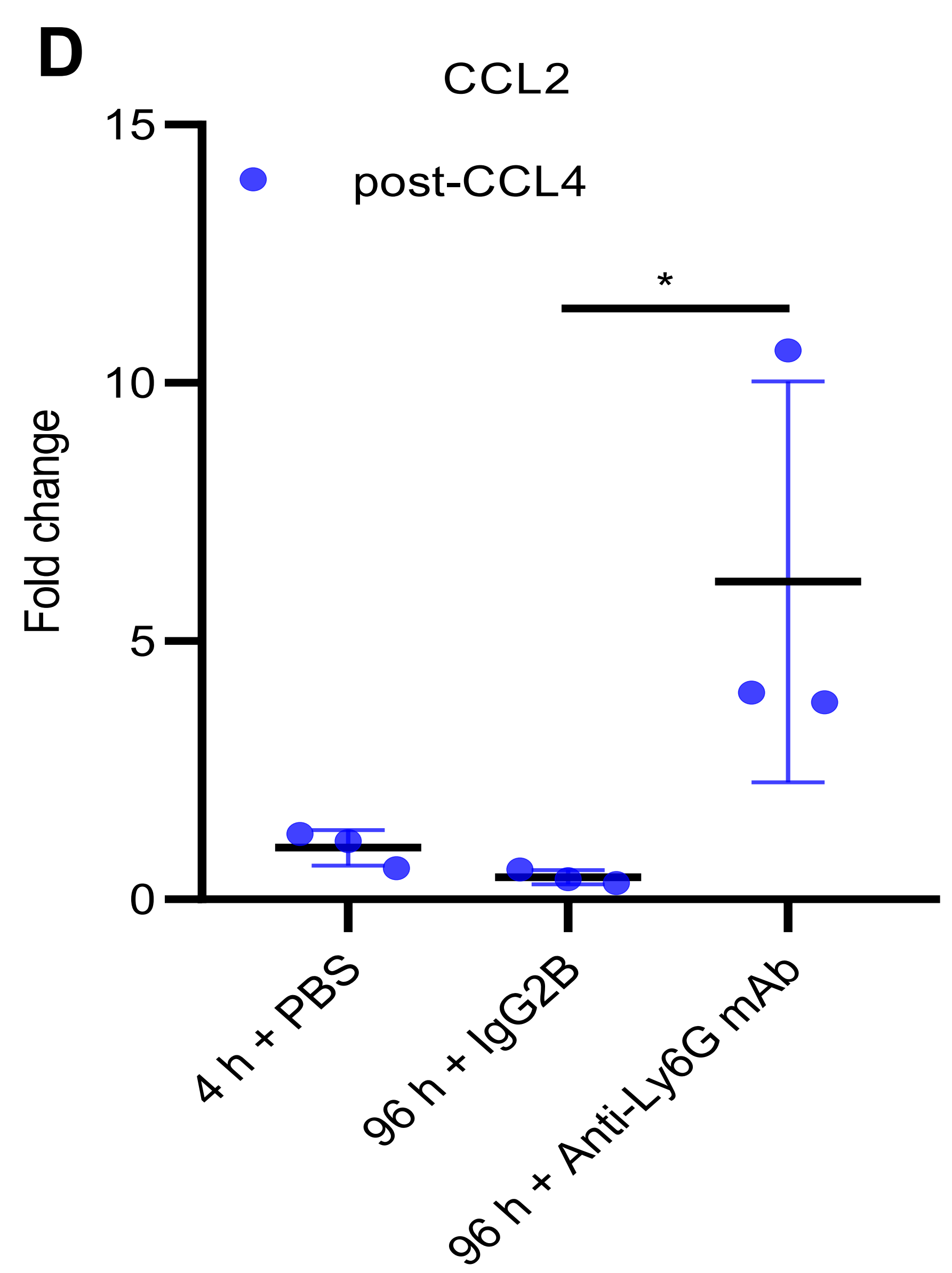
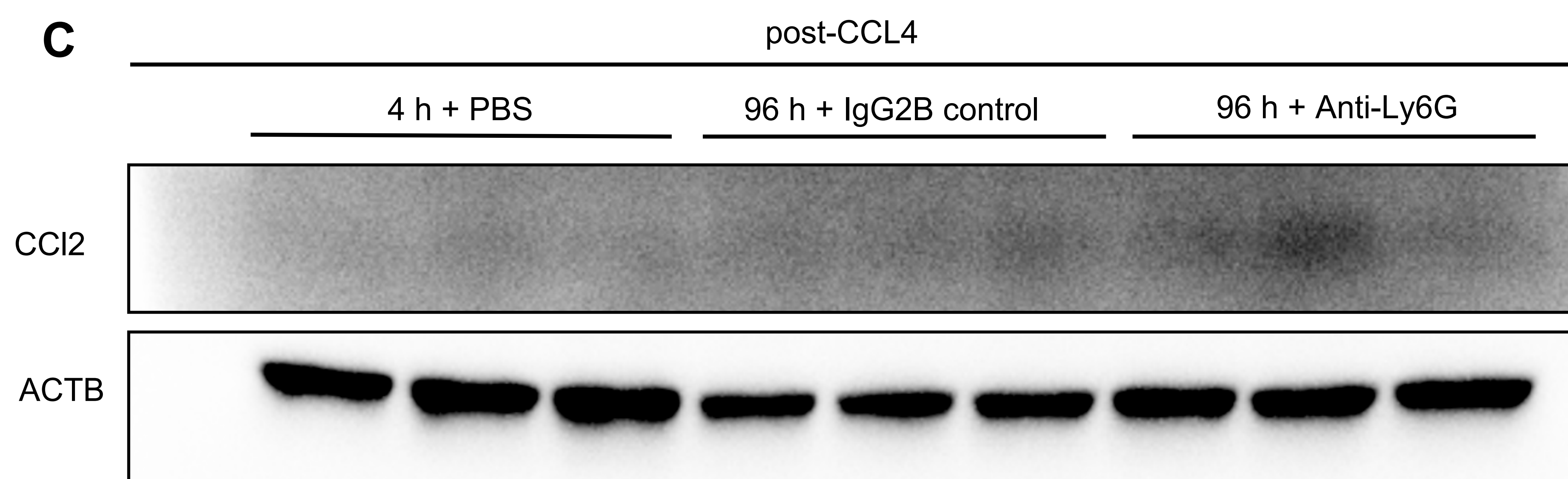
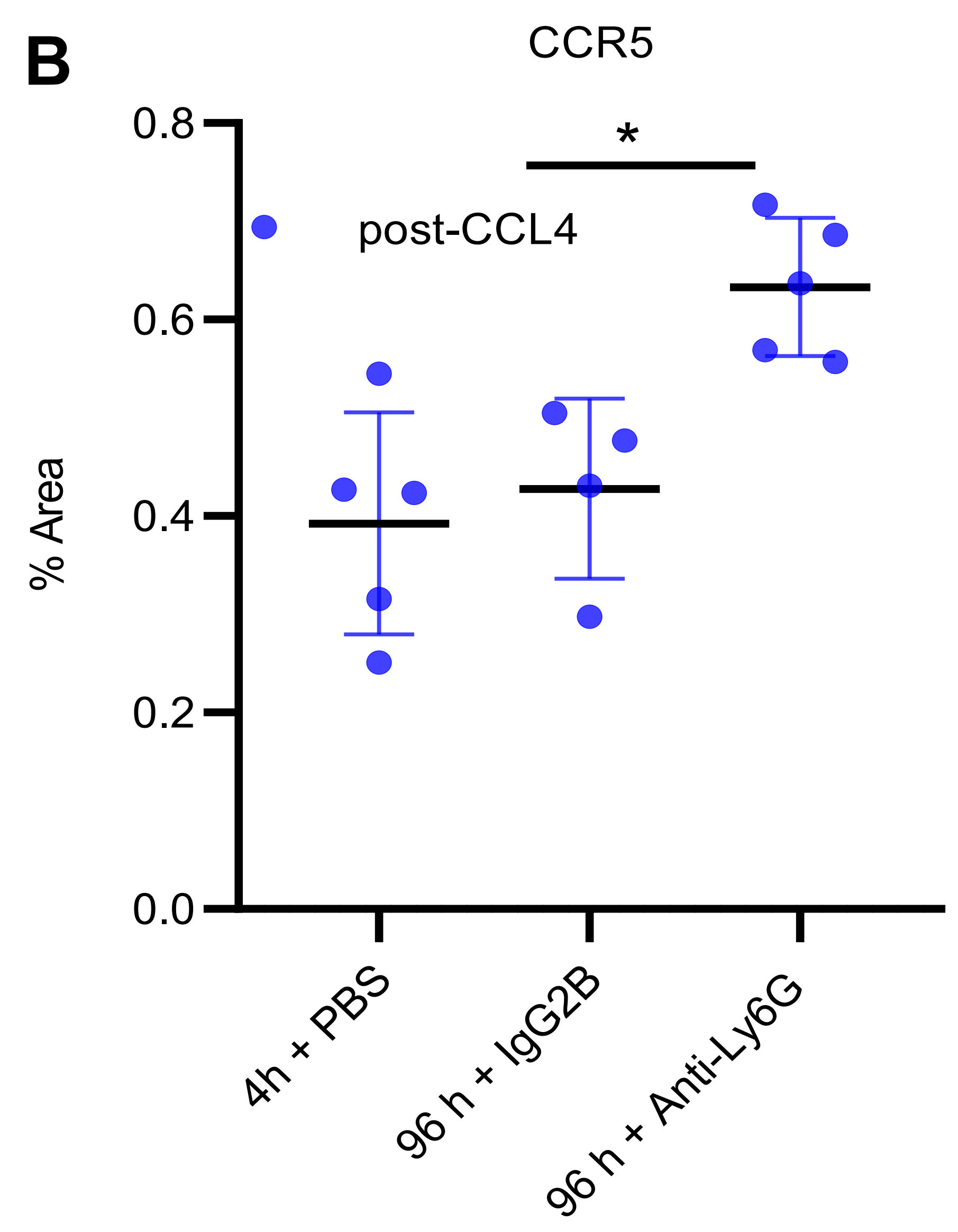
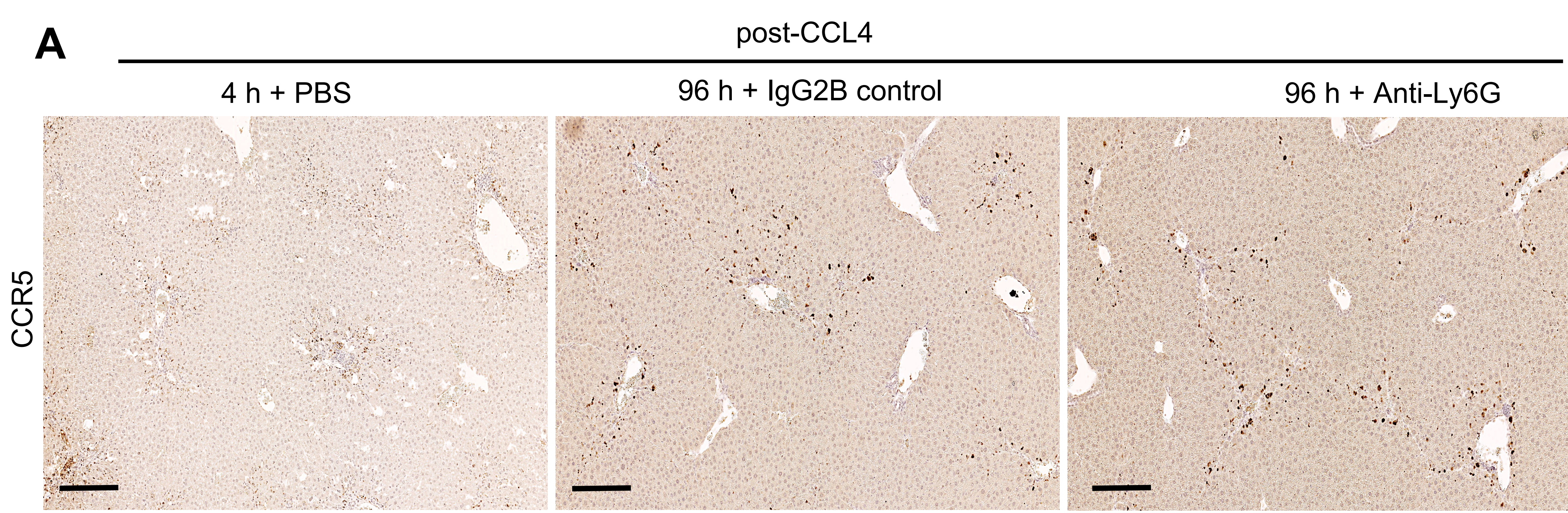


Supplementary Figure 2 (A) Representative Giemsa staining of blood smears of mice in experiment from **Supplementary Figure 3**. Black arrows indicate stained granulocytes. Scale bars= 100 μ m. **(B)** Number of granulocytes per field counted manually in 10 randomly selected images; n= 3 .**** P <0.0001, two-tailed unpaired t-test. Data are shown as means \pm SD **(C)** Representative immunohistochemical images of liver neutrophils (CD177 positive). White arrows point to CD177 positive cells (neutrophils), while black arrows highlight background. Scale bars=100 μ m

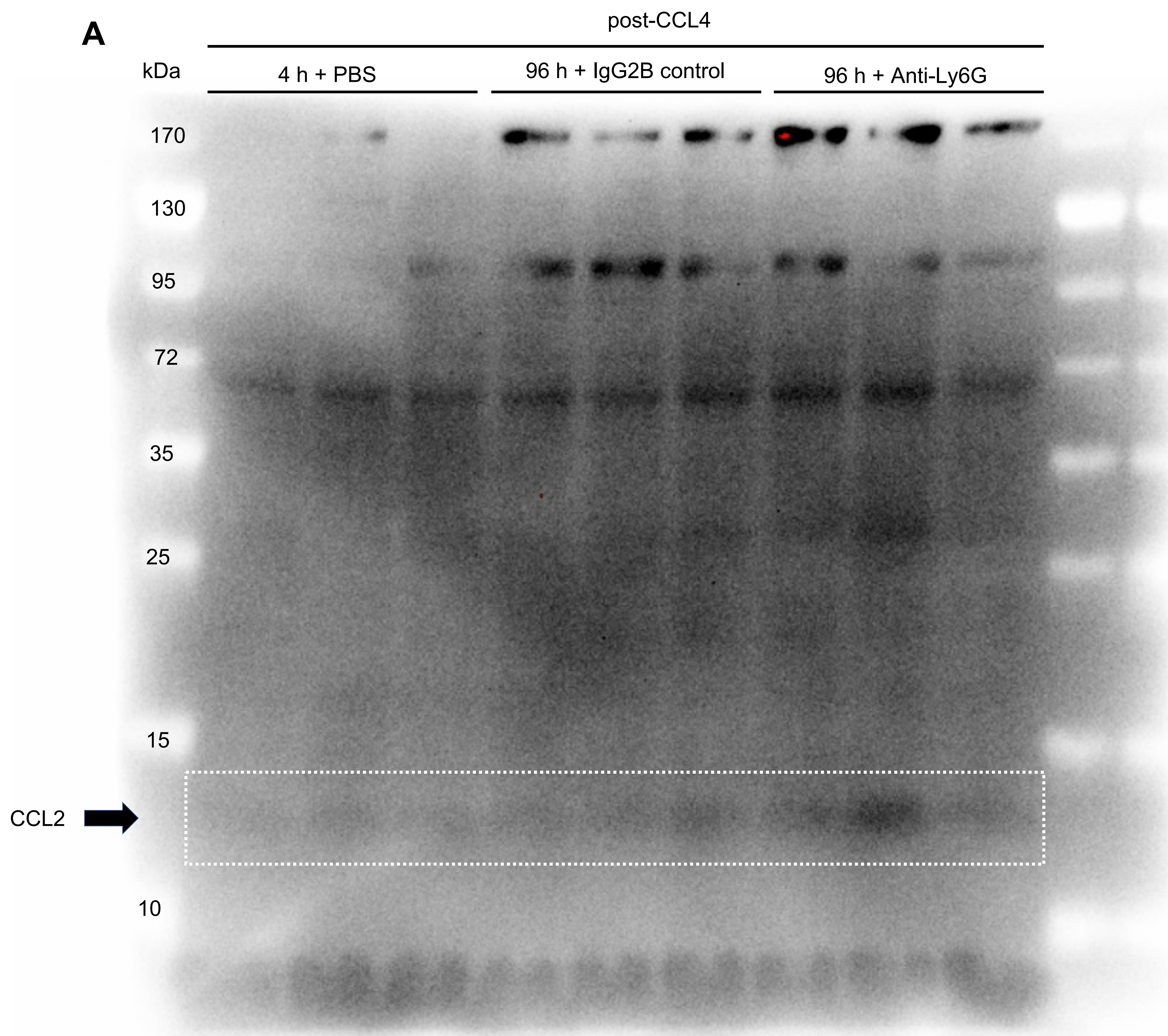


Supplementary Figure 3 The clone 1A8 of anti-Ly6G mAb worsens the spontaneous resolution of inflammation and fibrosis similarly to clone clone RB6-RC5 (A) Representative micrographs of liver sections from mice of experiment performed as shown in Figure 1A but using clone 1A8 instead of RB6-RC5 . Total collagen is stained with Sirius Red and total macrophages and activated HSCs with F4/80 and anti- α SMA mAb, respectively. Scale bars= 100 μ m (B-D) Percentage of area positive for Sirius Red, F4/80 or α SMA in 10 aleatory selected pictures calculated by Image J; n=3-5, * P <0.05; ** P <0.01, one-way ANOVA. Results are displayed as means \pm SD, n=3-5.

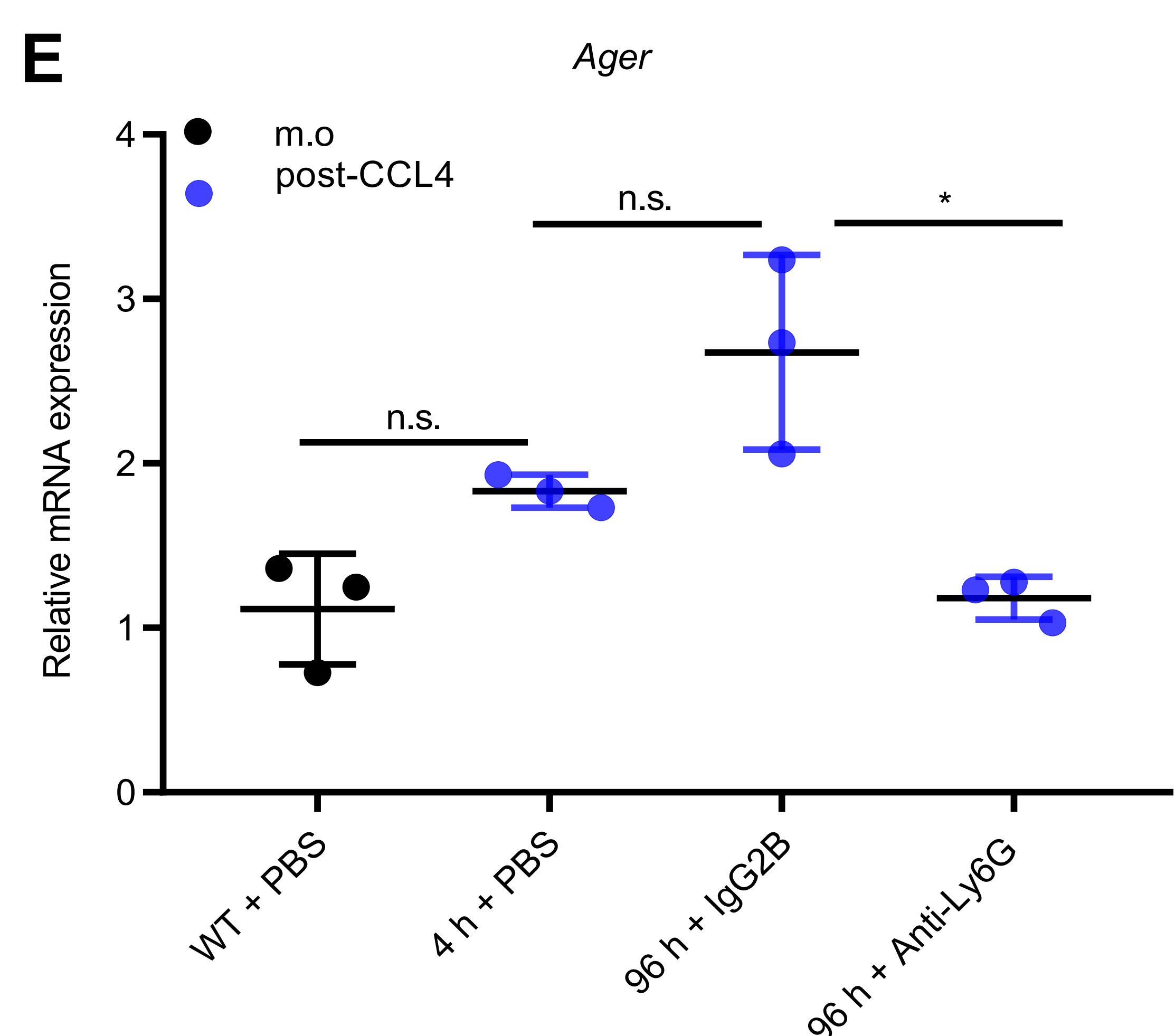
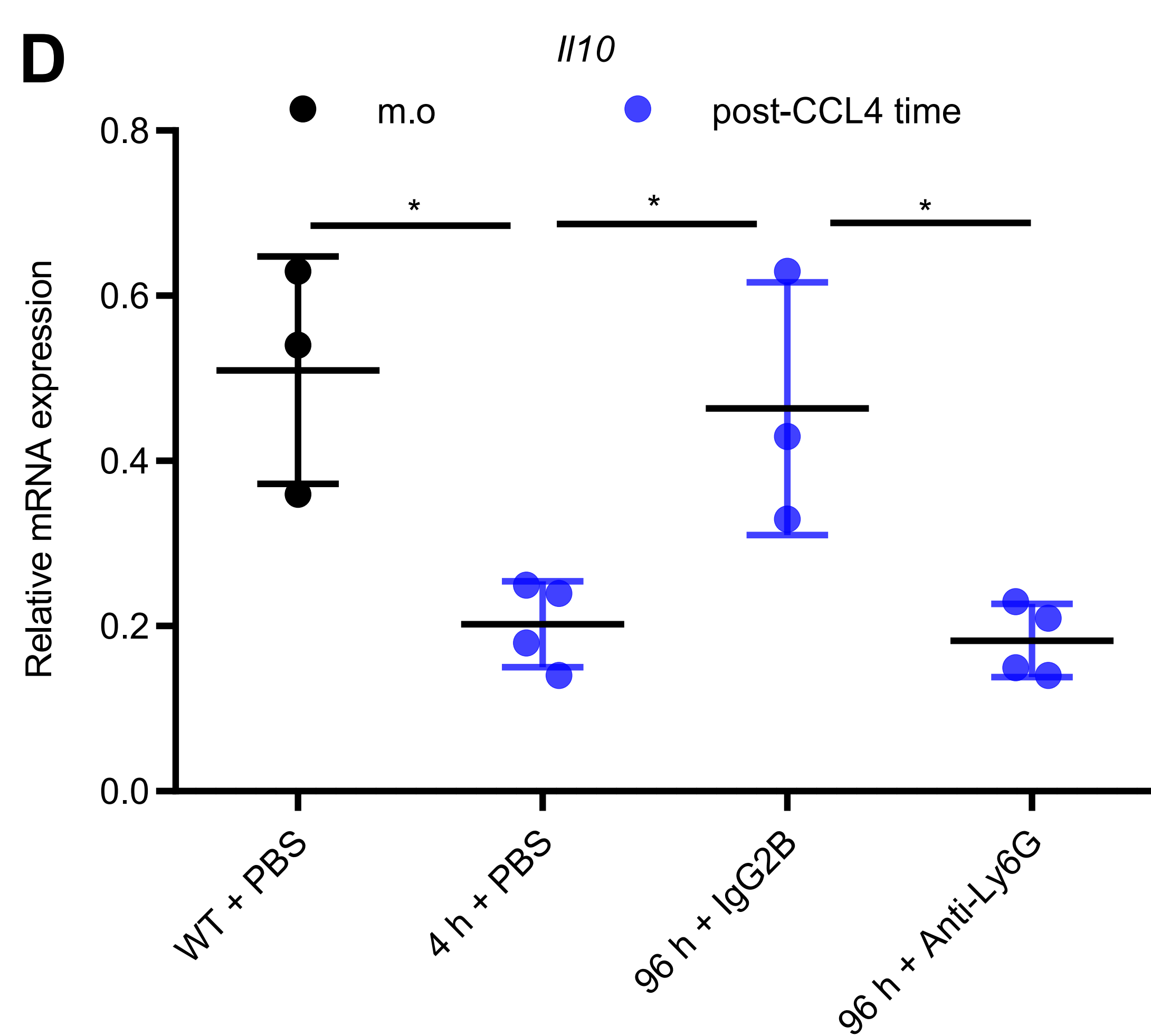
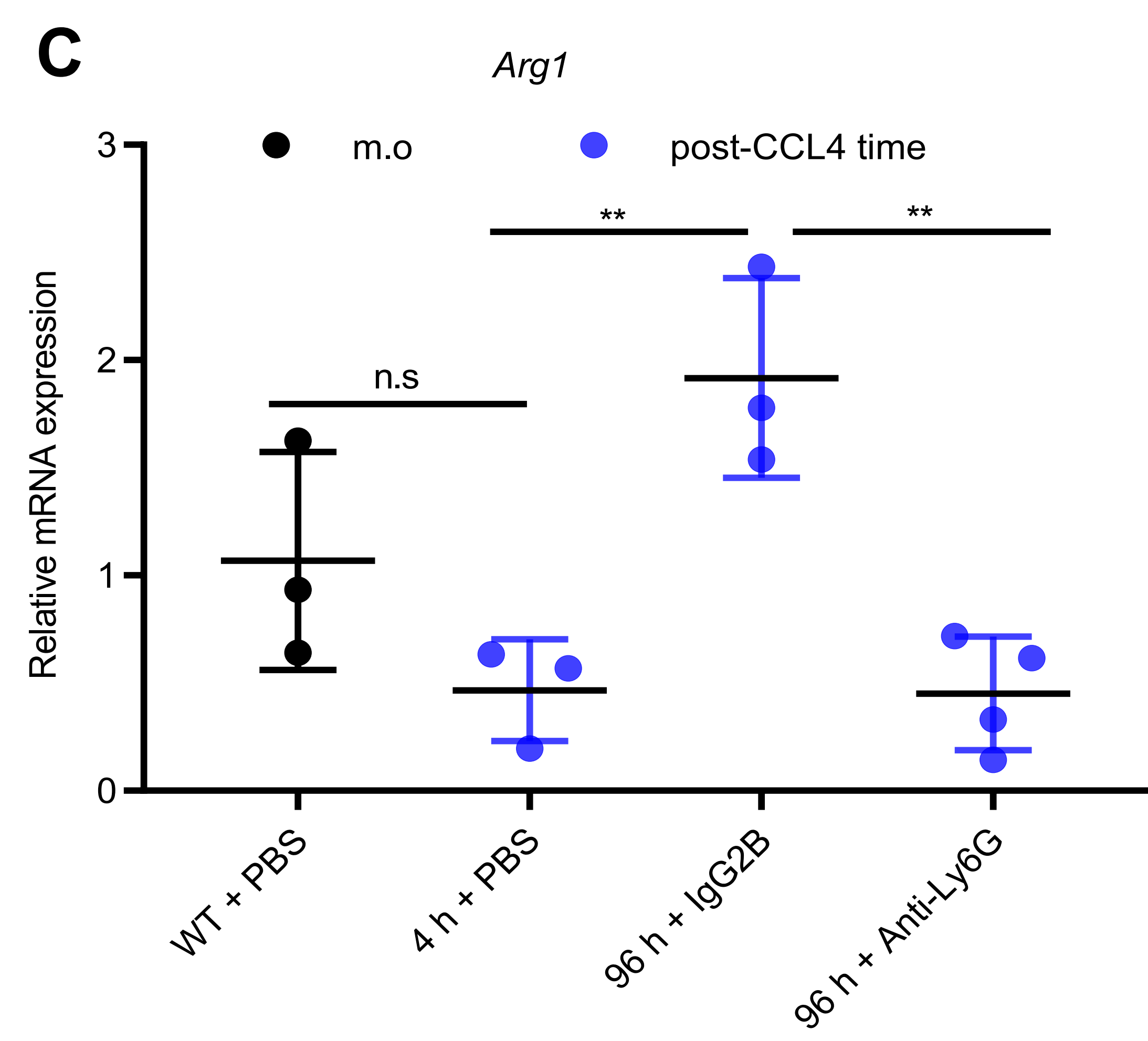
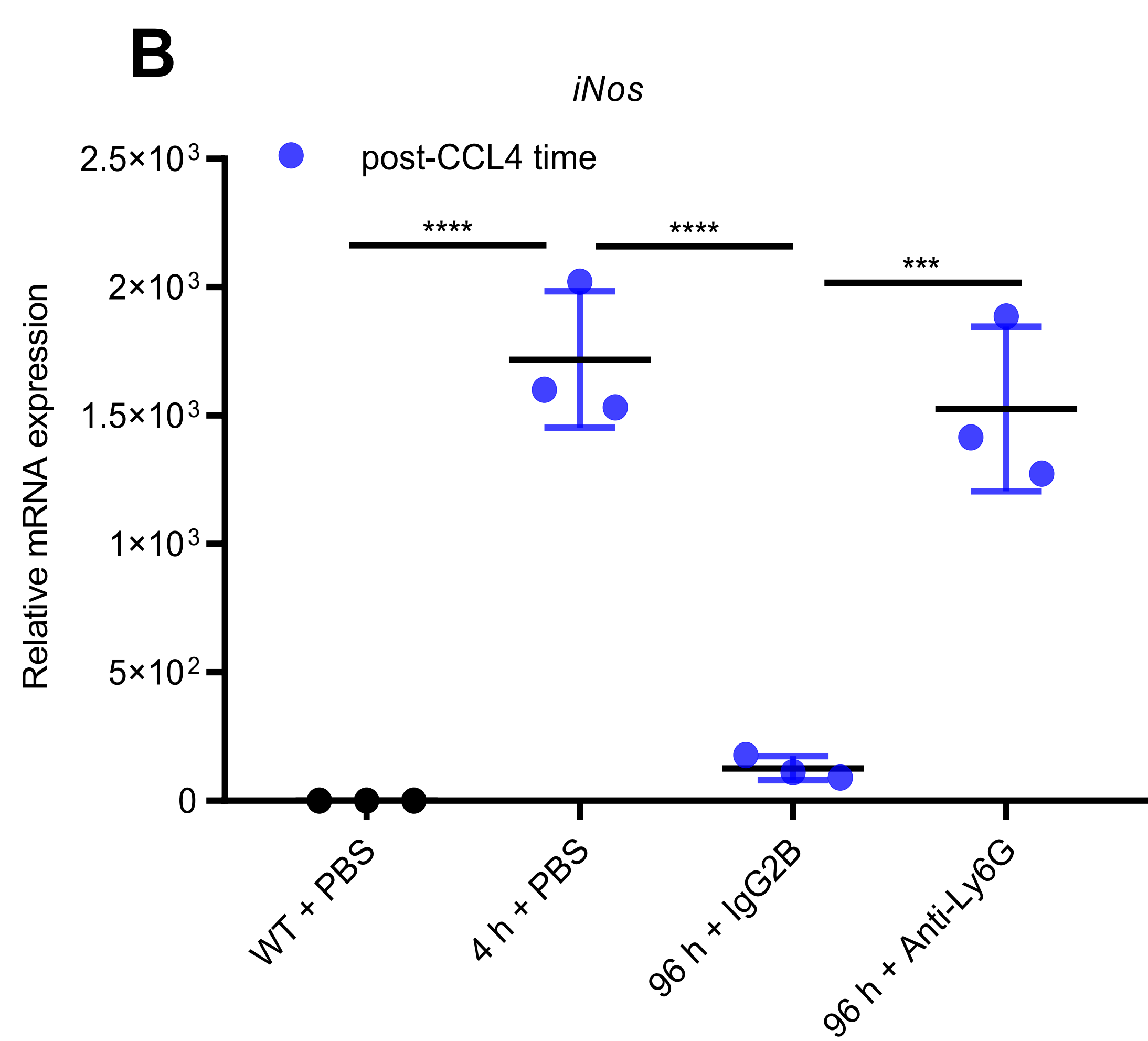
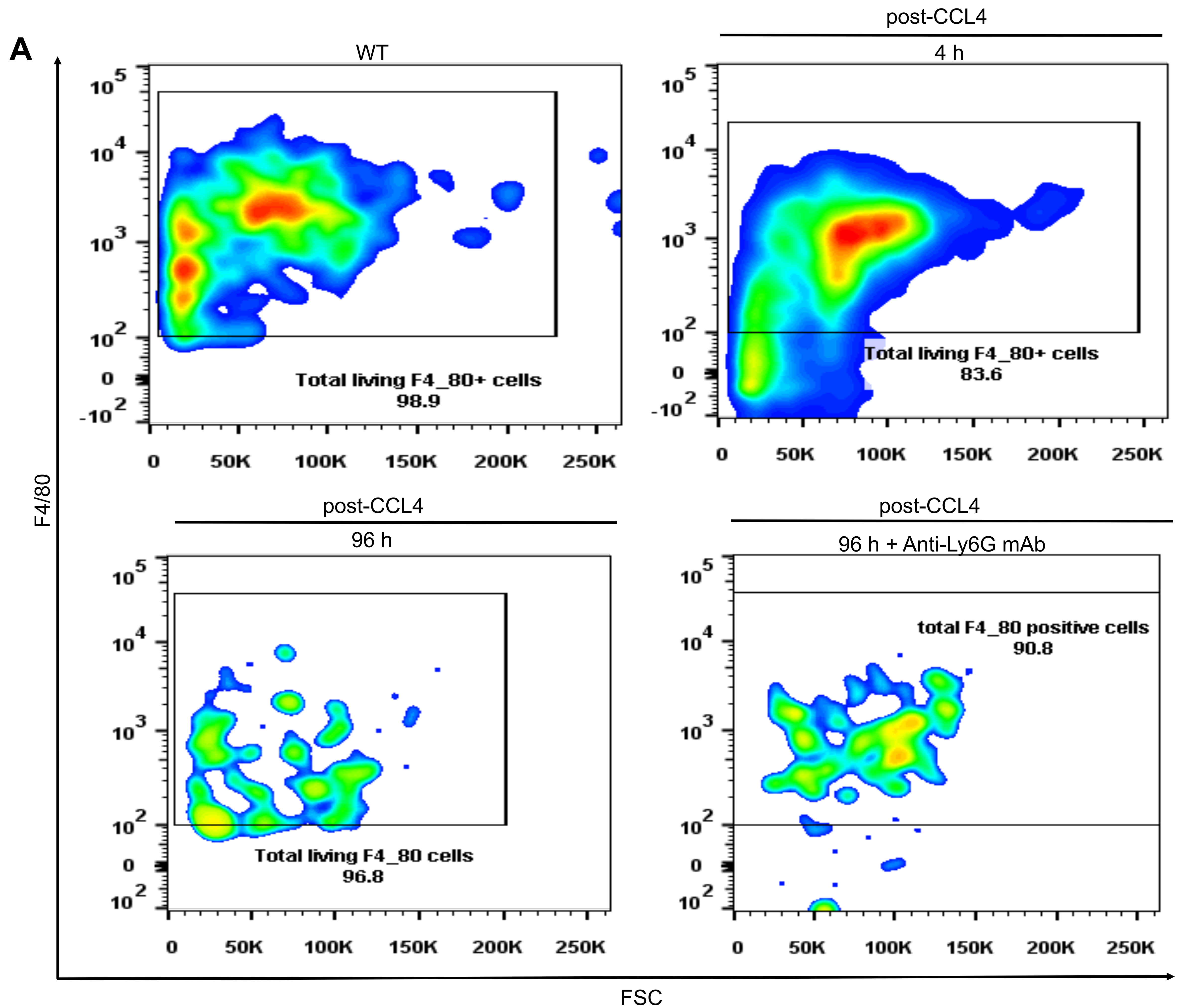




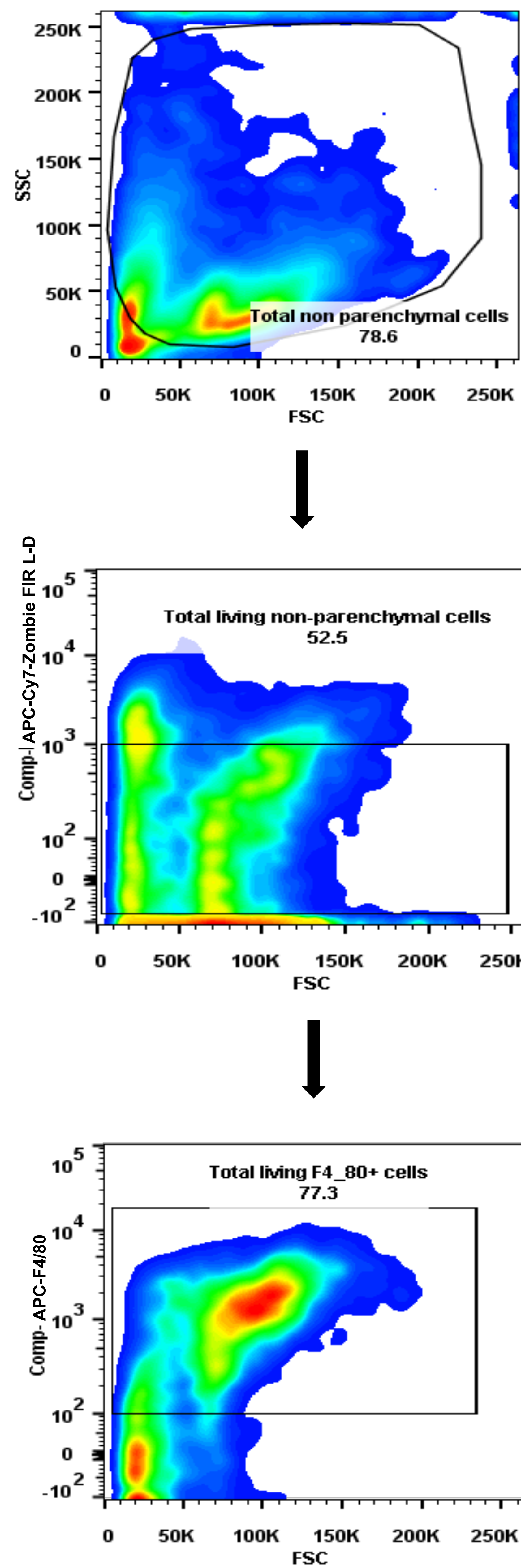
Supplementary Figure 4 Neutrophil depletion increases the CCR5 or CCL2 in SRLI (A) Representative micrographs of liver sections from mice of experiment performed as shown in Figure 1A. CCL3 and CCL4 responsive pro-inflammatory macrophages are shown by staining with CCR5 antibody. Scale bars= 100 μ m. **(B)** Percentage of area positive for CCR5 in 10 aleatory selected pictures calculated by Image J. * $P < 0.05$; one-way ANOVA. Results are displayed as means \pm SD; $n = 4-5$ **(C)** Western blot images of protein expression of CCL2 and the housekeeping protein ACTB. **(D)** Fold change of CCL2 protein expression as normalized by ACTB and calculated by Image J. One-way ANOVA. Results are shown as means \pm SD; $n = 3$.



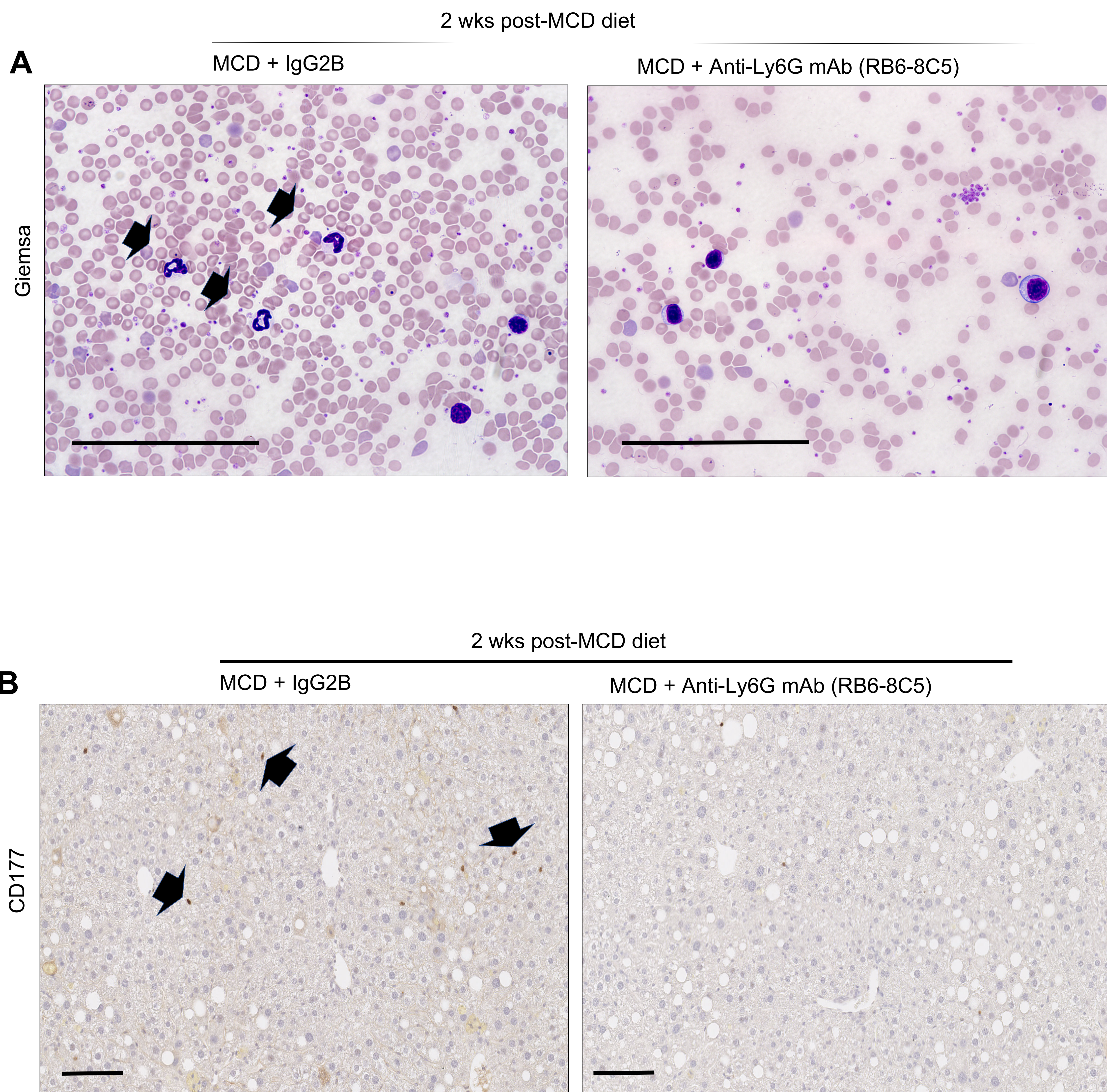
Supplementary Figure 5 Original, Uncropped WB image of CCL2 protein represented in Supplementary Figure 4.



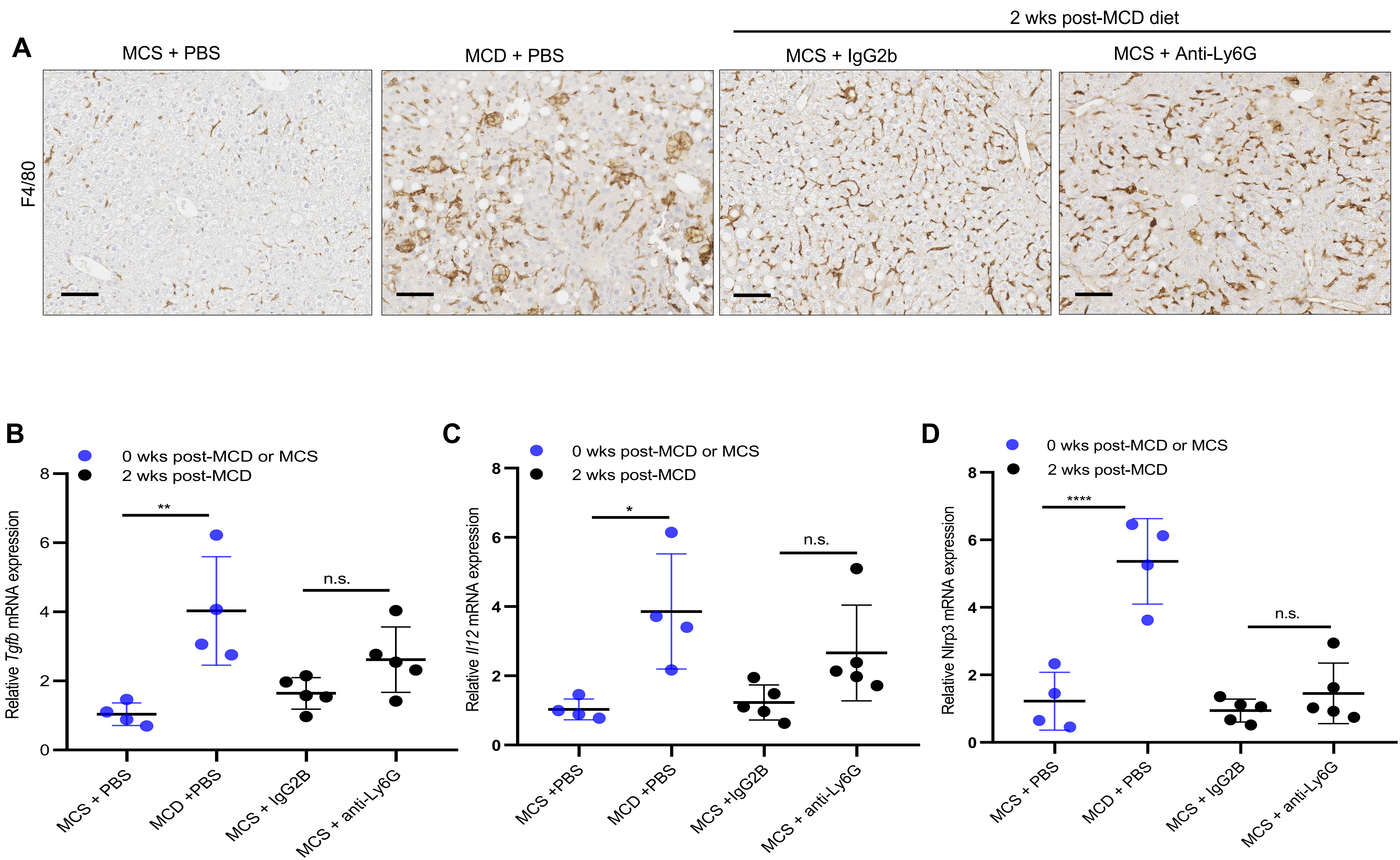
Supplementary Figure 6 Neutrophil depletion induces alternative hepatic macrophage activation during SRLI (A) Representative FACS analysis of F4/80 expression in macrophages isolated from the livers of experiment in **Figure 1 A** and stained with biotin anti-F4/80 (APC) mAb. Upper quadrants display F4/80 positive populations represented as percentages in legends where indicated. **(B-E)** Expression of *iNos*, *Arg1*, *Il10* and *Ager* mRNAs in liver macrophages from mice in **Figure 1 A** quantified by real time RT-PCR and normalized against *B2M* mRNA. Not significant (n.s.); * $P < 0.05$; ** $P < 0.01$; *** $P < 0.001$; **** $P < 0.0001$, one-way ANOVA. Results are expressed as means \pm SD, $n = 3-4$ /group.



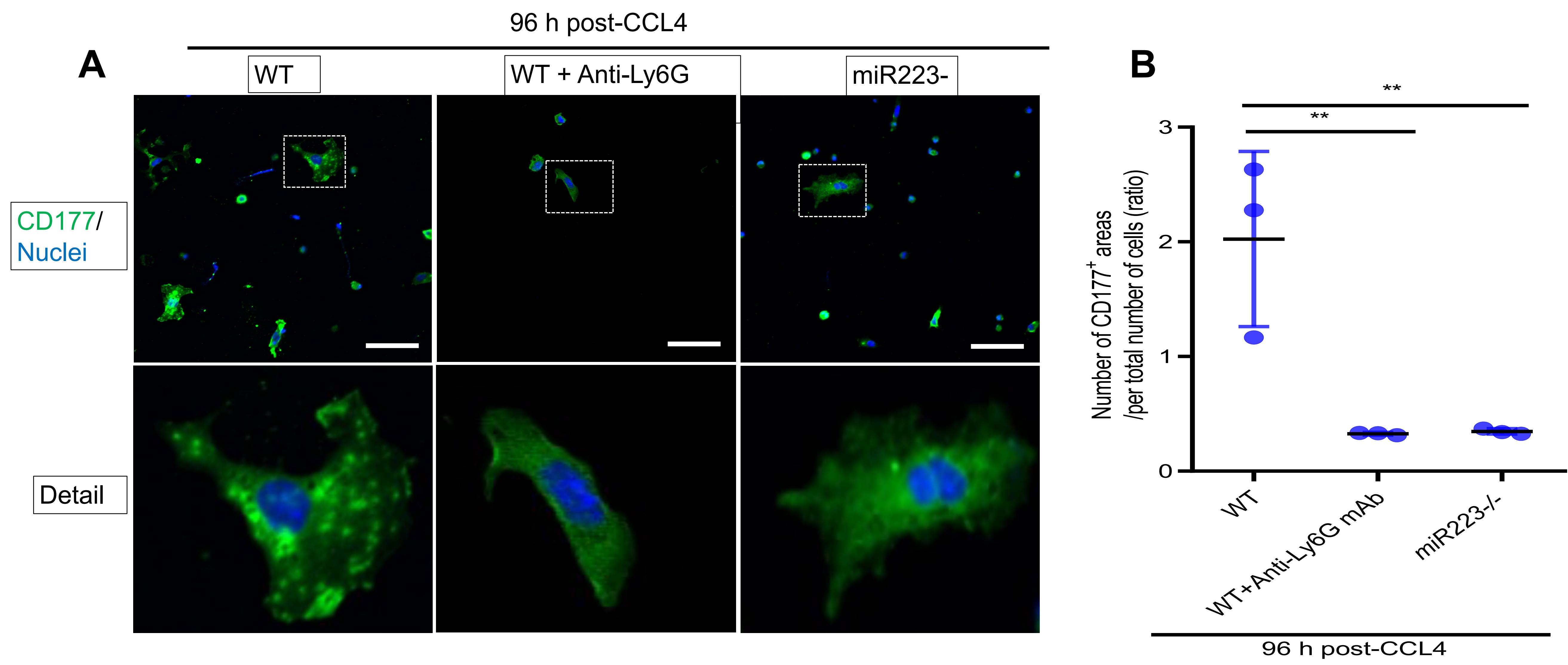
Supplementary Figure 7 Gating strategy followed in the FACS analysis of Supplementary Figure 2 A. (A) Total non-parenchymal cells were selected from the total population areas except axis adjacencies. Living non-parenchymal cells were selected as negative for APC-Cy7-Zombie FIR L-D. These cells were then gated for APC-F4/80 to select the positive population that represents the total living macrophages.



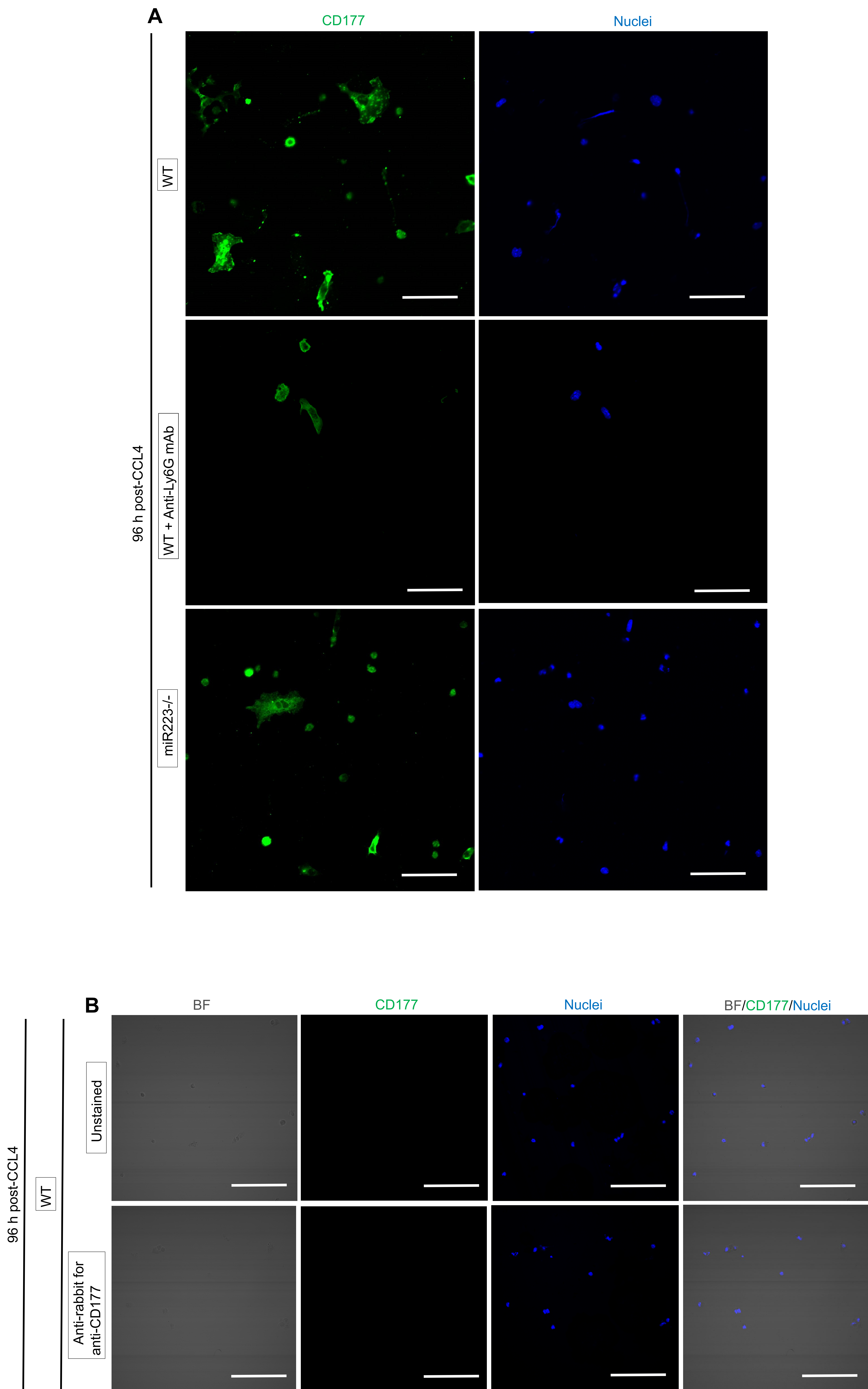
Supplementary Figure 8 (A) Representative Giemsa staining of blood smears of mice in experiment from **Figure 4 A**. Black arrows indicate stained granulocytes. Scale bars= 100 μ m. **(B)** Representative immunohistochemical images of liver neutrophils (CD177 positive). Black arrows point to CD177 positive cells (neutrophils). Scale bars=100 μ m



Supplementary Figure 9 Neutrophil depletion worsens spontaneous resolution of inflammation in NASH. (A) Immunohistochemical images of liver sections stained for macrophages (F4/80 positive). Scale bars=100 μ m. n=4-5 (B-D) Transcript levels of *Tgfb*, *Il2* and *Nlrp3* as measured by quantitative PCR and normalized by the housekeeping gene *B2m*; n=4-5. **** P <0.0001, One-way ANOVA. Data are shown as means \pm SD



Supplementary Figure 10 (A) Representative confocal immunofluorescent images of primary macrophages of livers from mice of **Figure 5 B** and **Figure 1 A**. DAPI staining for nuclei is represented in blue and staining with antibody for CD177 is shown in green. Dashed quadrants representing cells with areas positive for CD177 are amplified in the detail image. Scale bars= 100 m. **(B)** Number of CD177 positive areas normalized by the total number of cells per field and expressed as ratio in 12 randomly selected images quantified by computerized imaging. ** $P < 0.01$, one-way ANOVA. Results are displayed as means \pm SD, $n=3$.



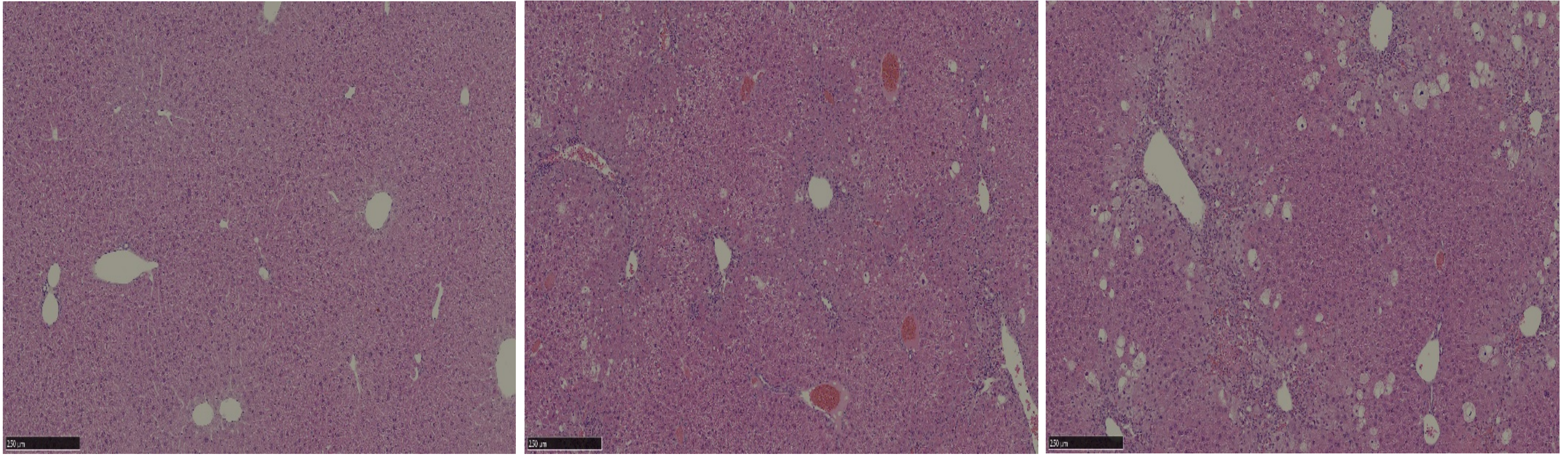
Supplementary Figure 11 (A) Individual merges of confocal immunofluorescent images showing CD177 positive areas and nuclei of hepatic macrophages from **Supplementary Figure 6** stained with anti-CD177 Ab and DAPI. Scale bars= 100 μ m. **(B)** Representative confocal pictures of primary hepatocytes from WT mice of experiment in **Supplementary Figure 10** unstained or stained with only Alexa Fluor 488 anti-rabbit Ab and DAPI (nuclei) to test the specificity of the anti-CD177 Ab. Scale bars= 100 μ m.

WT

WT

miR223^{-/-}

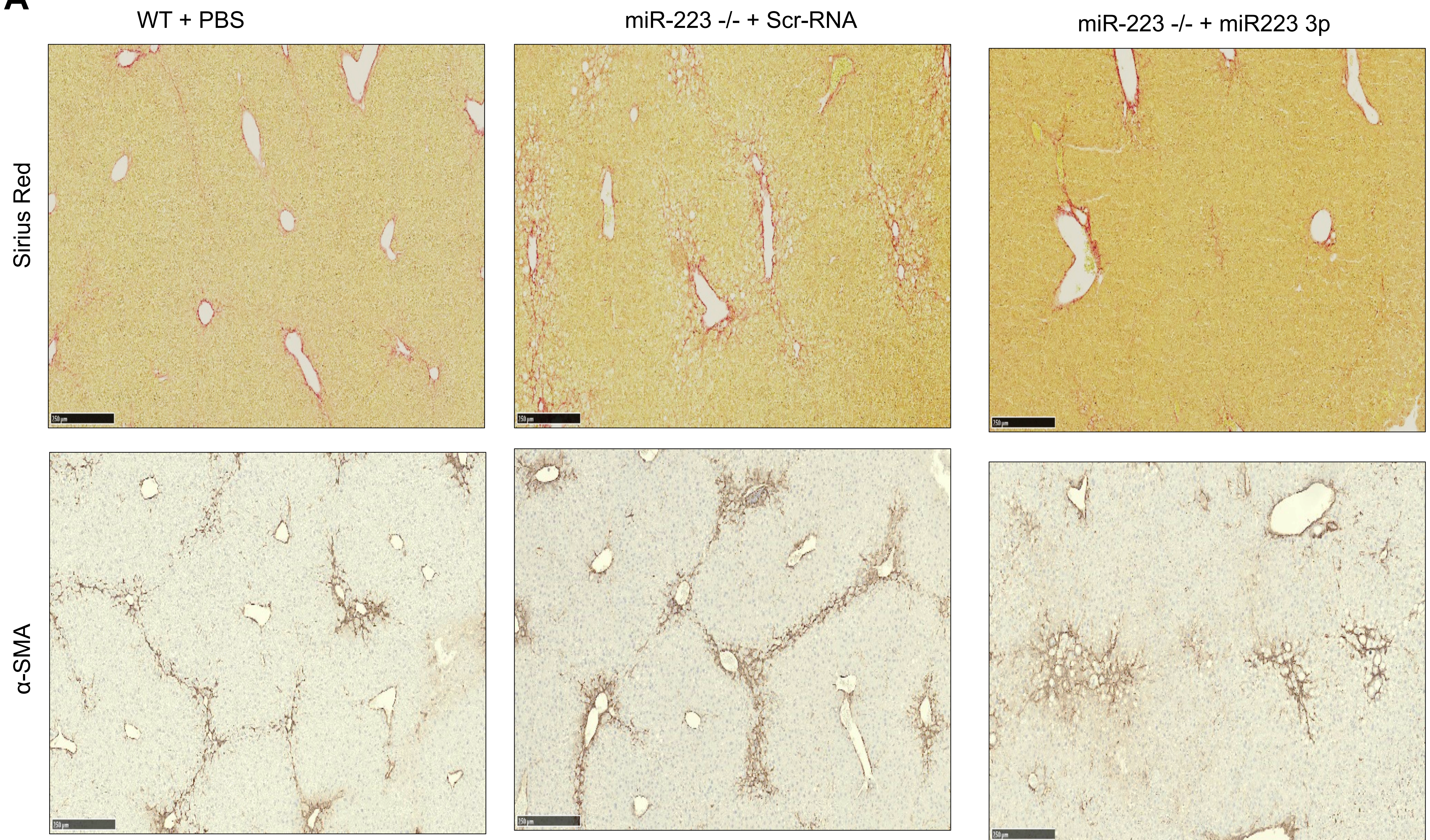
H & E



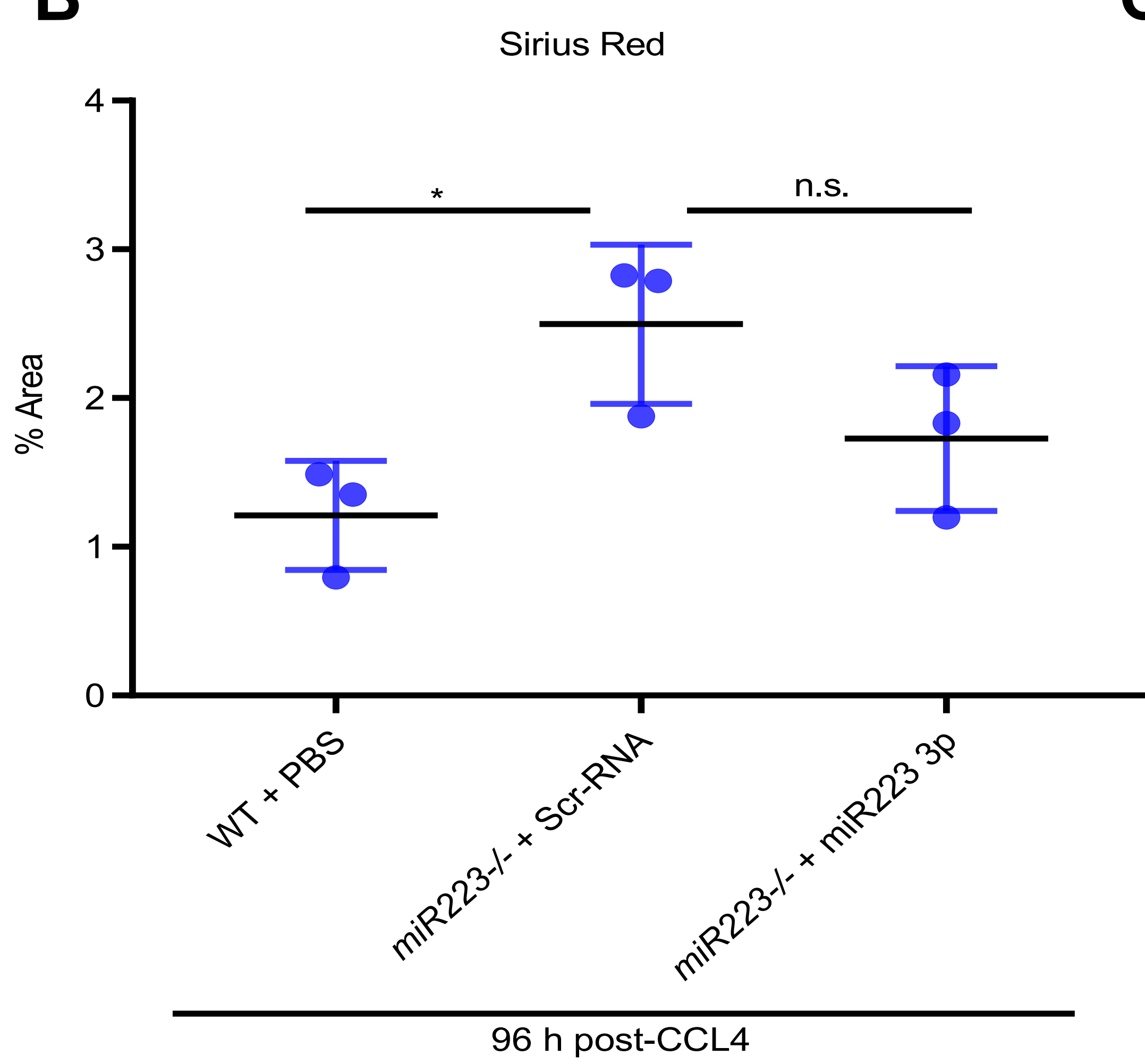
Supplementary Figure 12 (A) Representative images of parenchymal and non-parenchymal cells in liver sections from mice of **Figure 5 B** stained with H & E. Scale bars=100 μ m

96 h post-CCL4

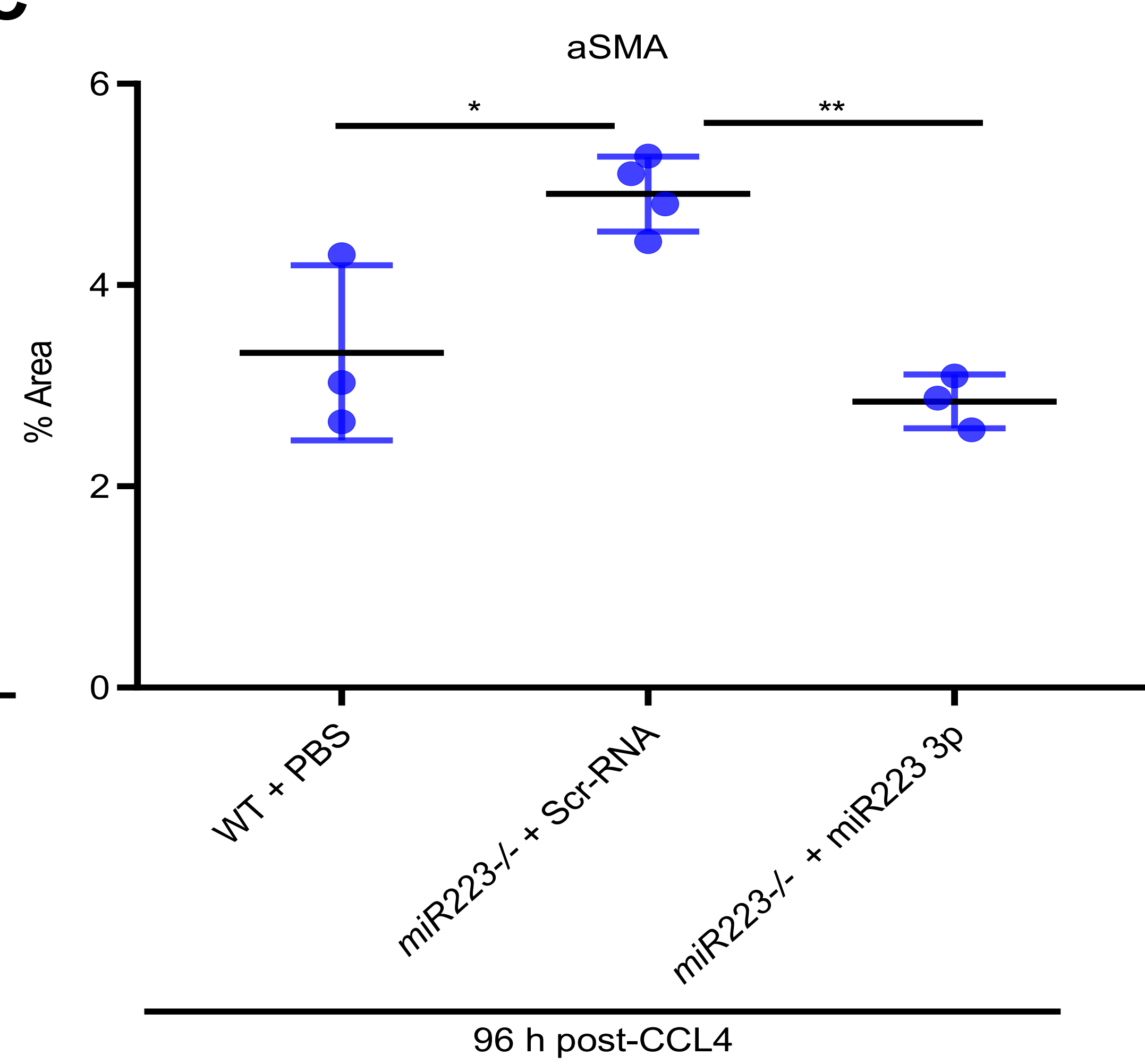
A



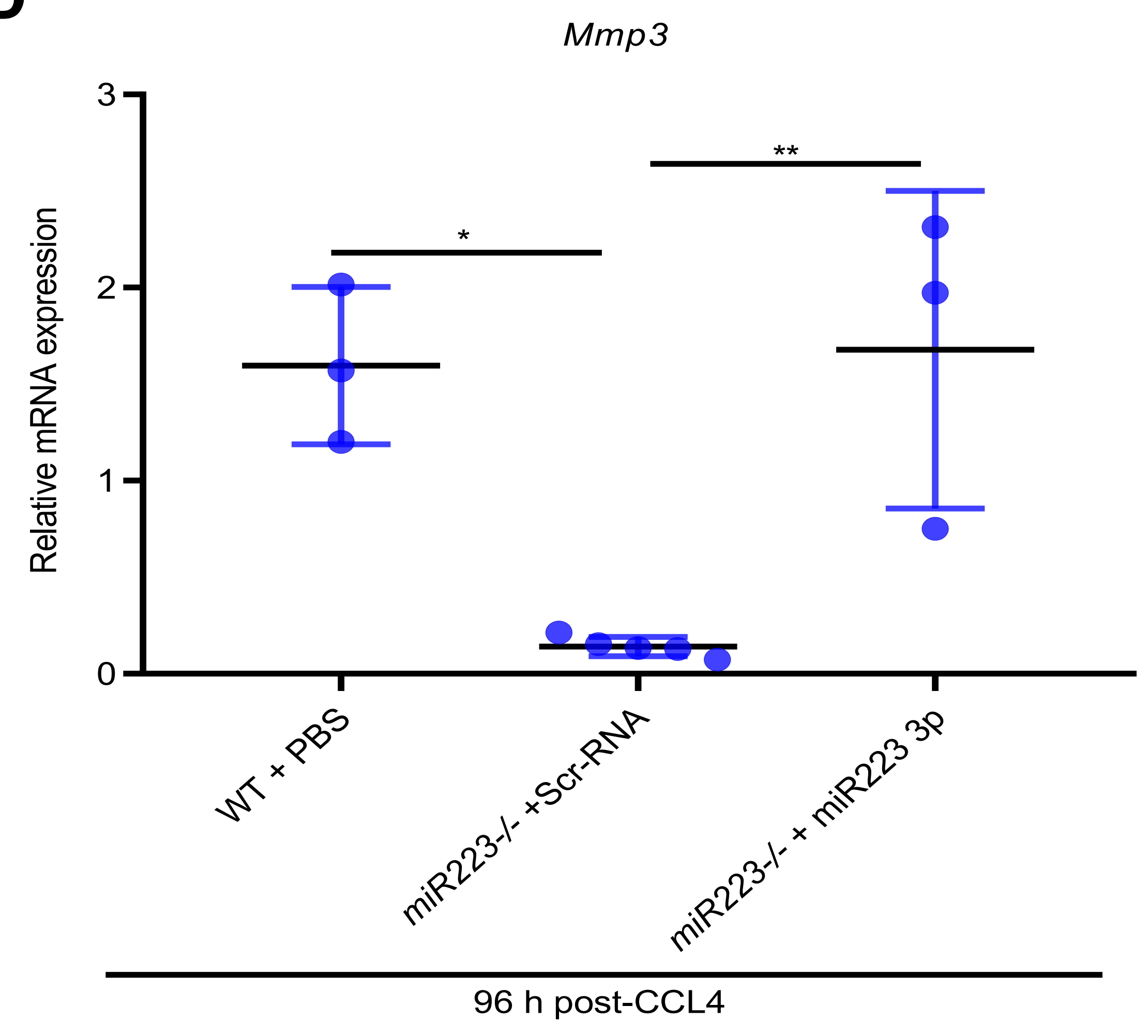
B



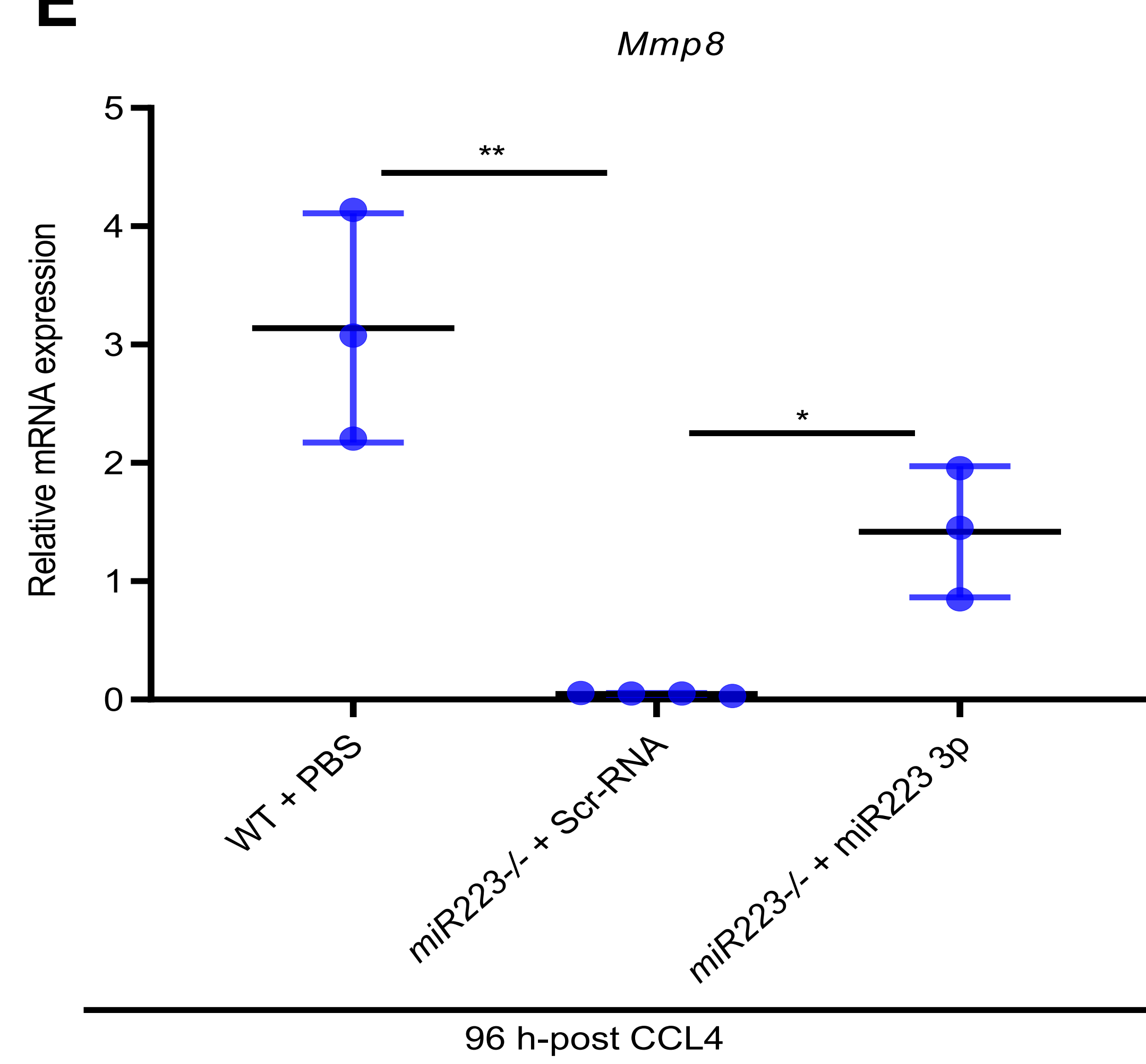
C



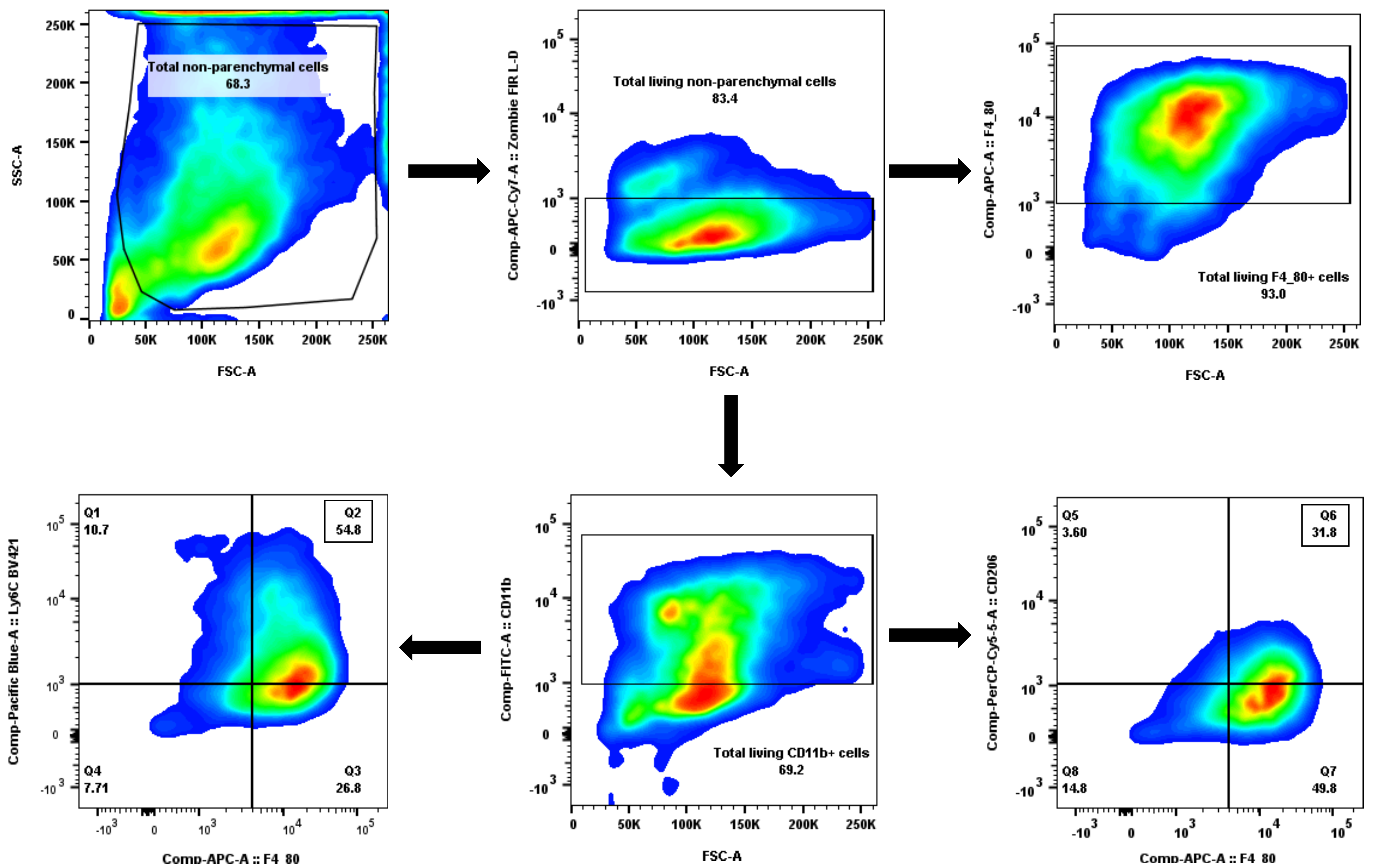
D



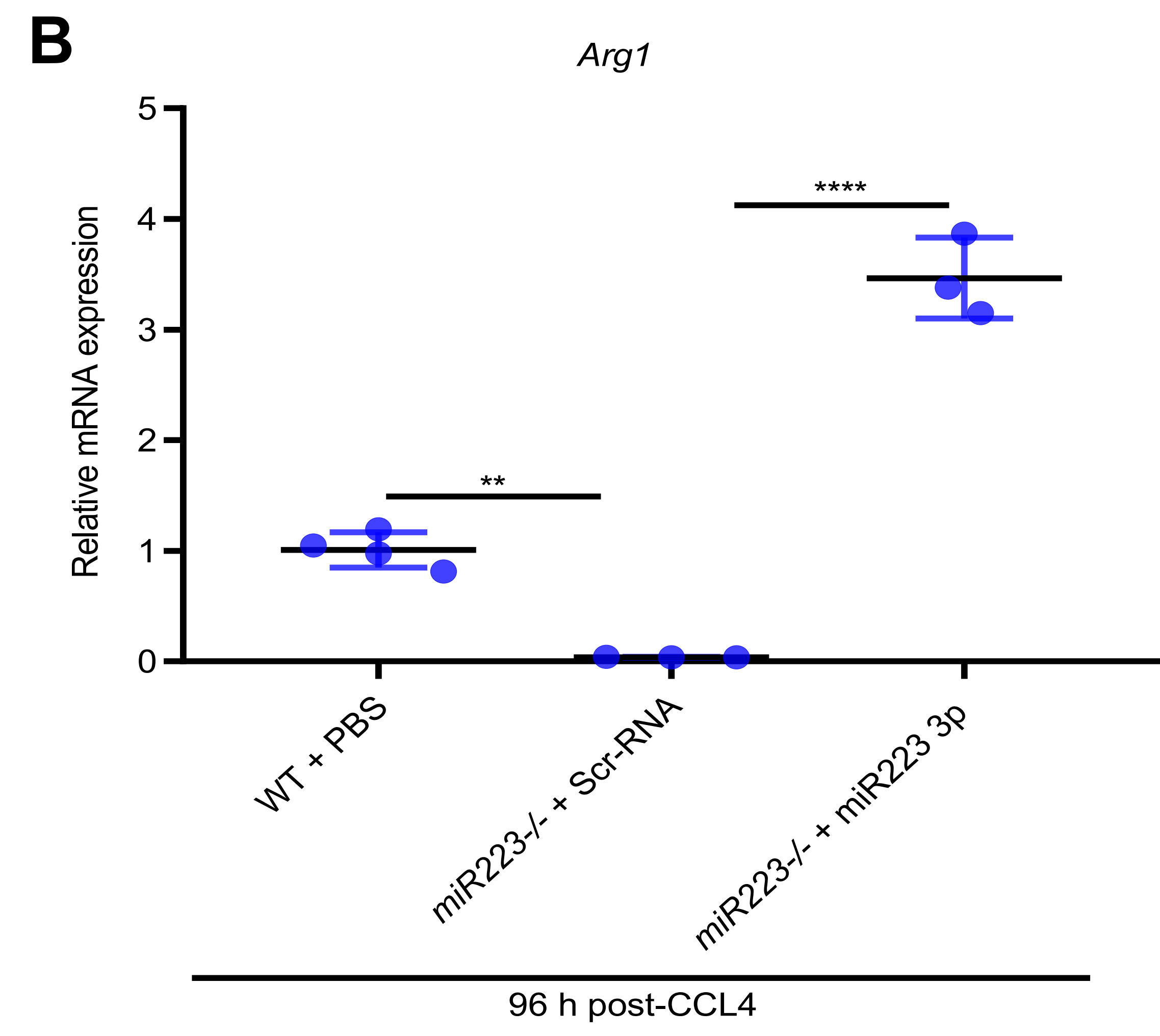
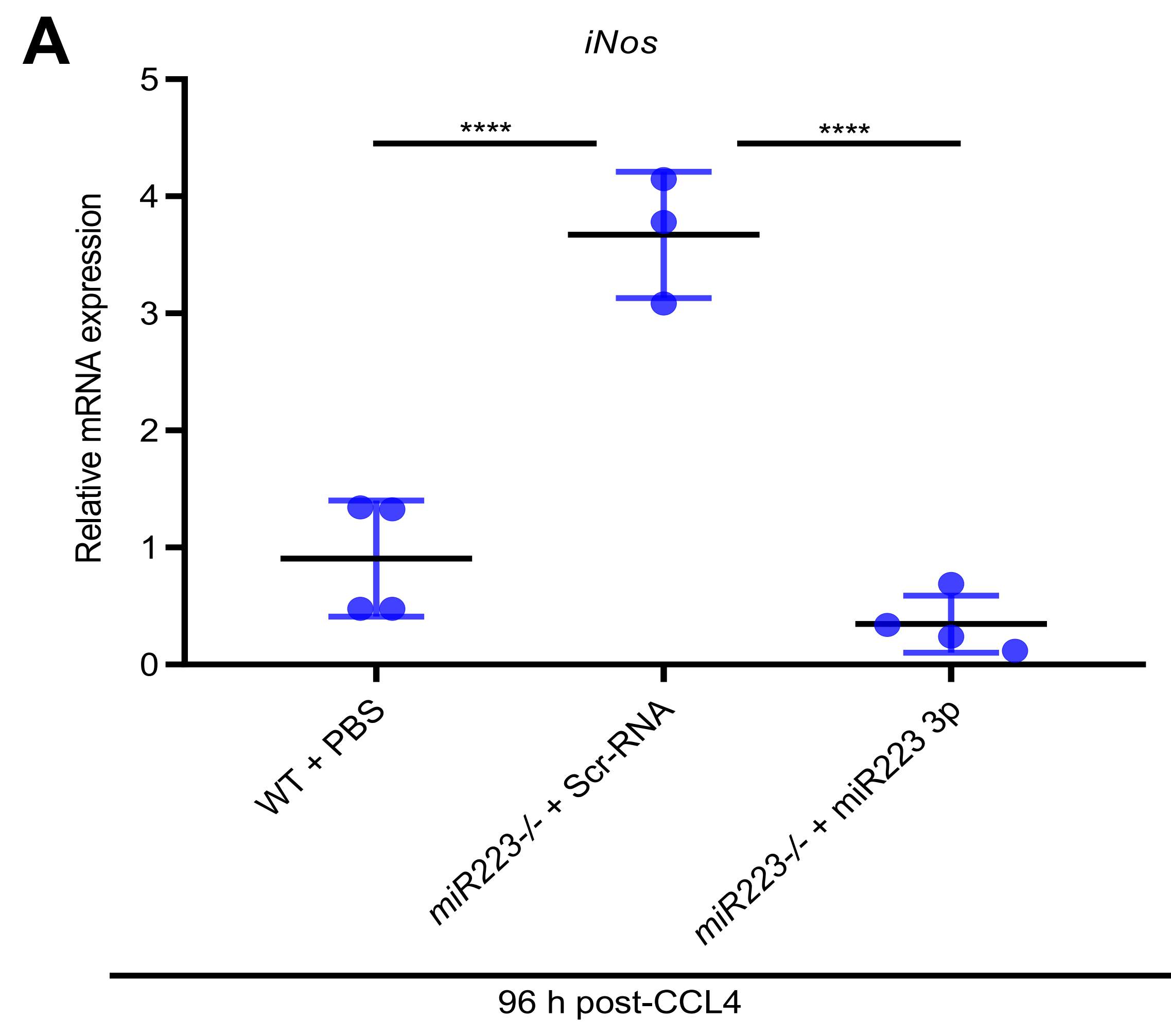
E



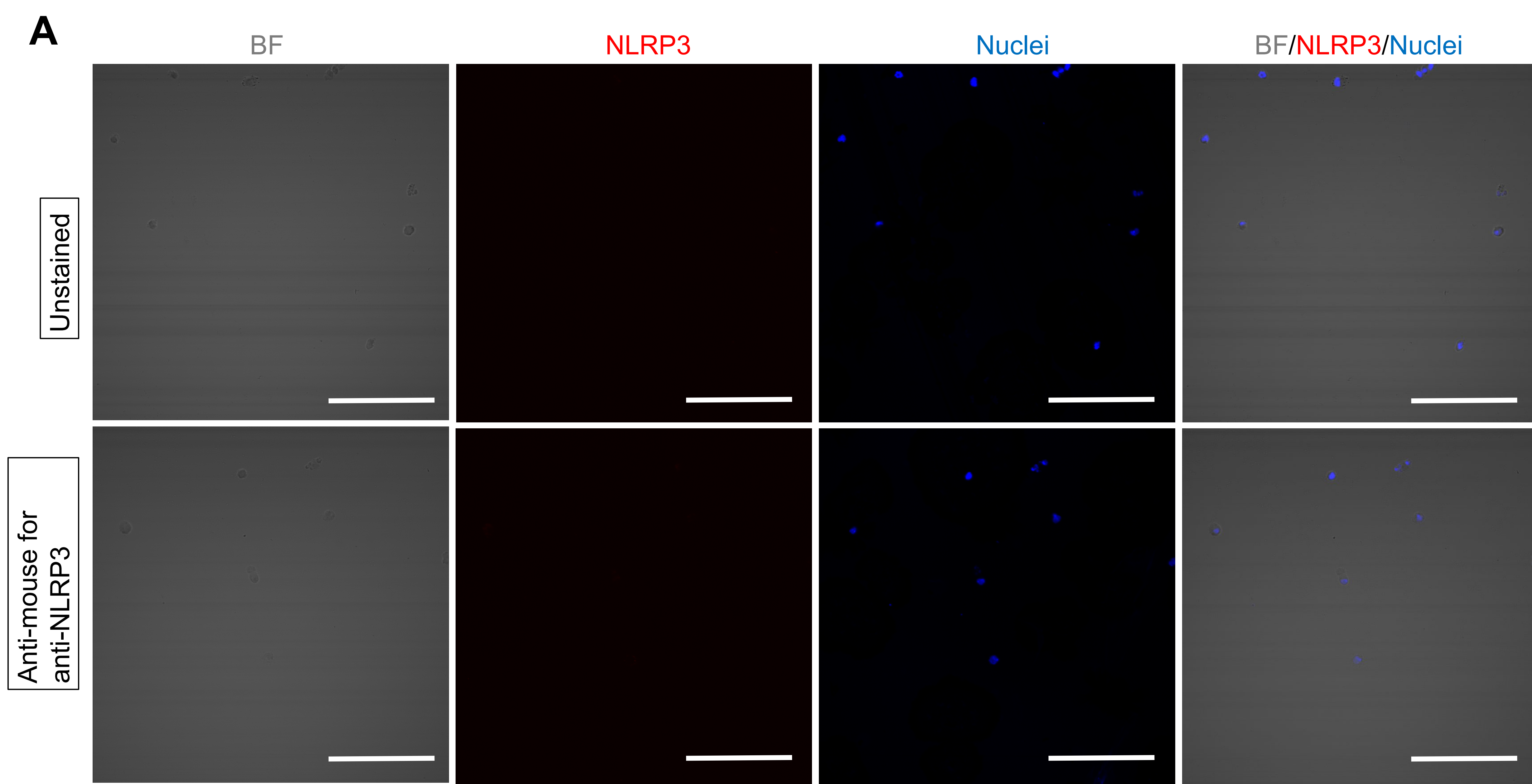
Supplementary Figure 13 miR-223 deficiency worsens spontaneous resolution of early liver fibrosis (A) Representative immunohistochemical images of liver sections from mice of experiment in **Figure 5 B**. Total collagen is stained with Sirius Red and activated HSCs with anti- α SMA mAb. Scale bars= 100 μ m (**B-C**) Percentage of area positive for Sirius Red and α SMA in 10 aleatory selected pictures calculated by Image J; n= 3-5/group (**D-E**) Expression of *Mmp3* and *Mmp8* mRNAs normalized by *B2m* mRNA and measured by real time RT-PCR; Not significant, * P <0.05; ** P <0.01, one-way ANOVA. Results are displayed as means \pm SD, n=3-6.



Supplementary Figure 14 (A) Representative gating strategy of FACS analysis from **Figure 8 A**. Total non-parenchymal cells were selected from the total population area except axis proximities to exclude debris and artifacts. Total living non-parenchymal cells were selected as negative for APC-Cy7-A-Zombie FIR L-D. From this population, cells positive for APC-A-F4/80 were selected to determine the purity of the total living macrophage population after using biotin F4/80 mAb in the MACS isolation procedure. Total living-nonparenchymal cells were also gated for FITC-A-CD11b to establish a hallmark positive population of living macrophages. From this population, pro-inflammatory and restorative macrophages were selected as double positive cells for Pacific Blue-A-Ly6C BV421/APC-A-F4/80 or PerCP-Cy5.5-A-CD206/APC-A-F4/80, respectively.

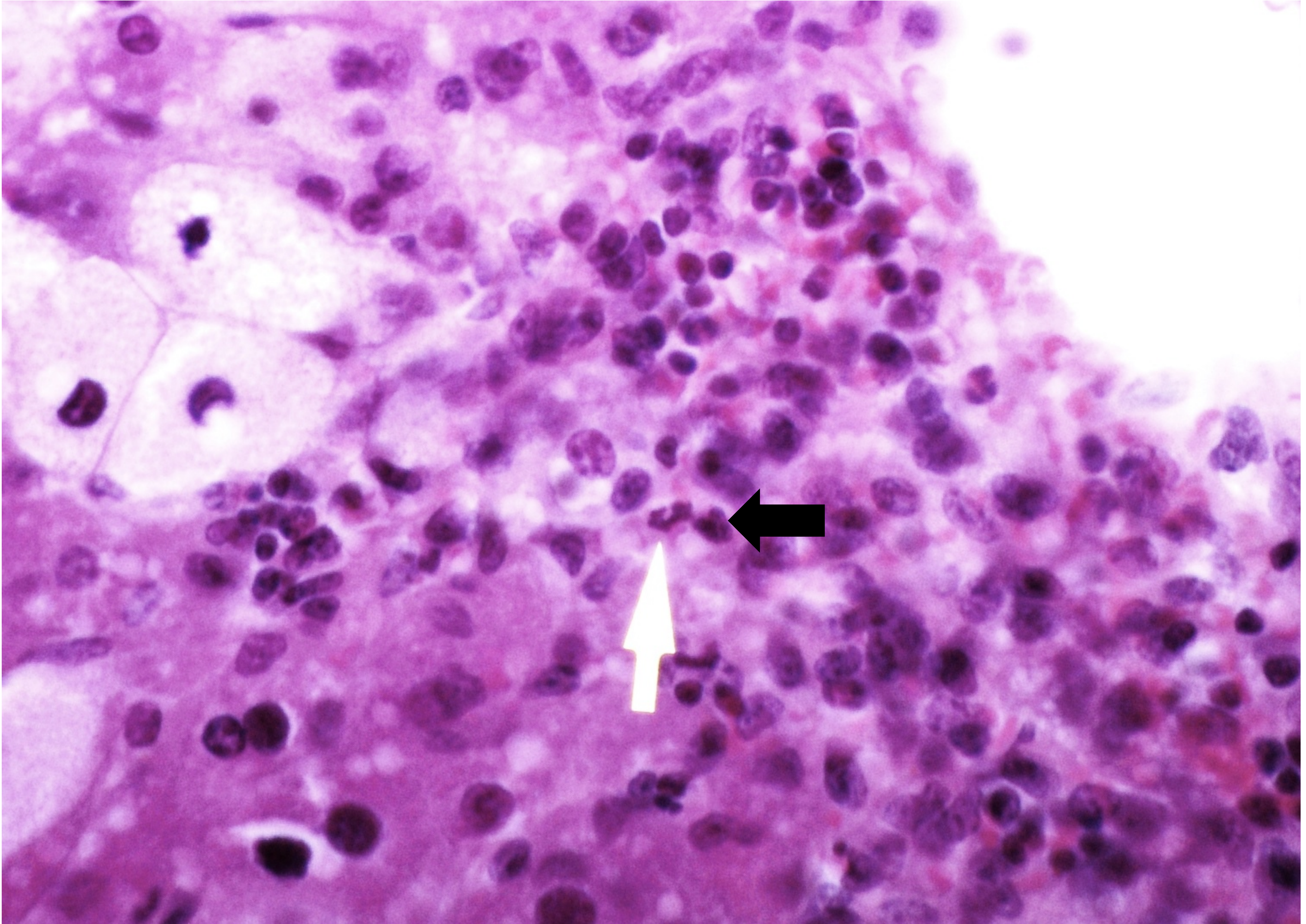


Supplementary Figure 15 (A-B) Expression of *iNos* and *Arg1* mRNA in primary hepatic macrophages of mice from experiment in **Figure 5 B** normalized to *B2m* mRNA and measured by real time RT-PCR. ** $P < 0.01$; **** $P < 0.0001$, one-way ANOVA. Data are shown as means \pm SD, $n = 3-4$ /group

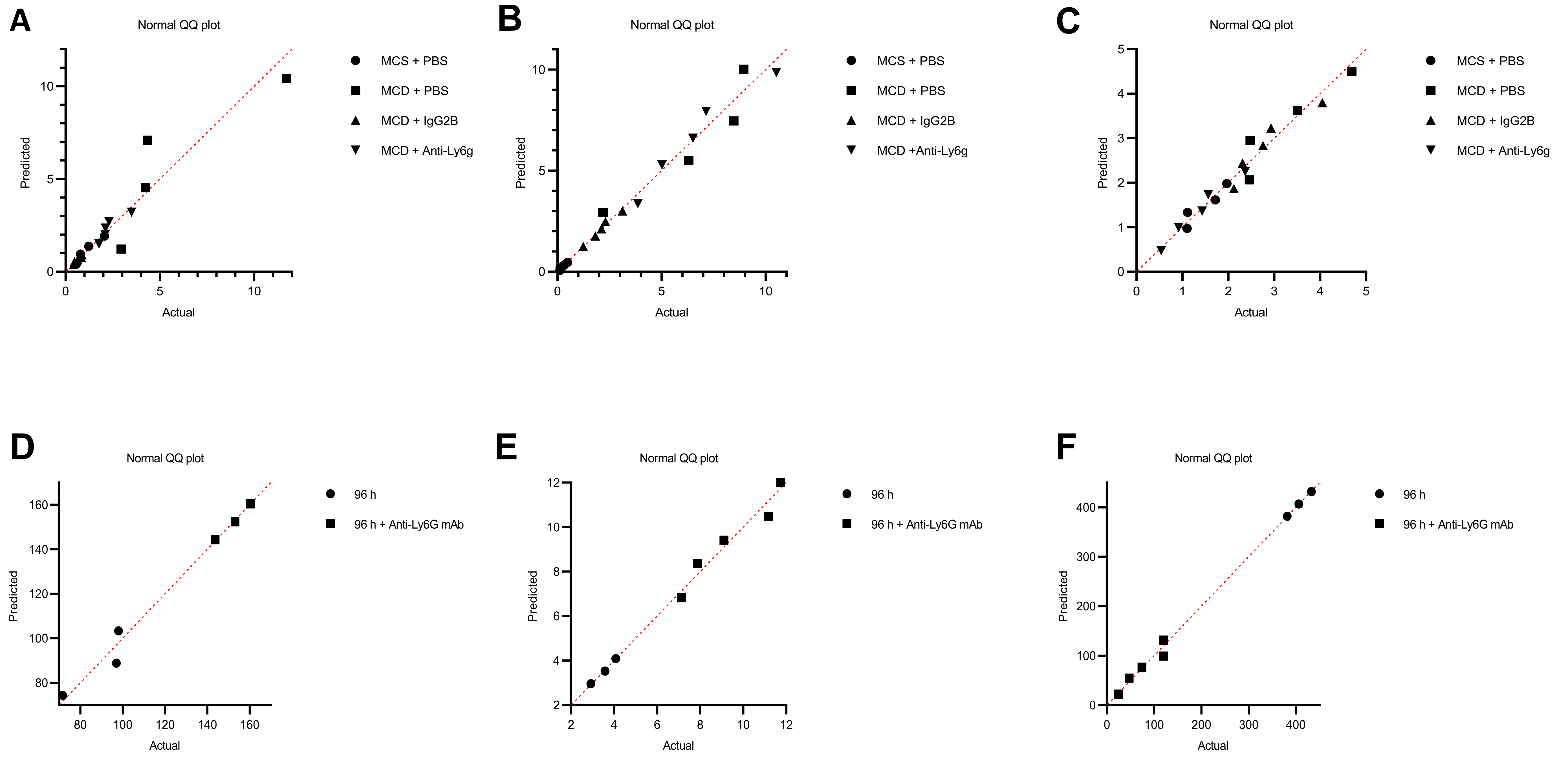


Supplementary Figure 16 (A) Representative confocal images of hepatic macrophages from WT mice of experiment in **Figure 9 C** unstained or stained with only Alexa Fluor 598 anti-mouse Ab and DAPI (nuclei) to test the specificity of the anti-NLRP3 Ab. Scale bars= 100 μ m.

96 h post-CCL4



Supplementary Figure 17 (A) Representative H & E staining of liver slides from non-antibody treated, CCL4-intoxicated mice showing the proximity of granulocytes and monocytes as highlighted by the white (granulocyte-like cell) and black arrow (monocyte-like cell).



Supplementary Figure 18 Representative data normality analysis. A-C corresponds to panels C-E of Figure 4 (significances analysed by One-way ANOVA); D-F represent B and F-G of Figure 1 (significances analysed by two-tailed, unpaired t-Test). Shapiro Wilk test (alpha=0.05) was used to check normal Gaussian distribution.